A Hydraulic Model for the Prediction of Wash Load in Mountainous Drainage Basins

By Kazuo Ashida, Shinji Egashira and Tadayoshi Kanayashiki

(Manuscript received June 10, 1981)

Abstract

This study has been carried out to develop a hydraulic method for the prediction of wash load concentration during a runoff due to a rain fall. In order to develop such a method, efforts should be made on the following two problems: Where and how is wash load produced? How can the distribution of flow discharge be evaluated in a drainage basin? After one clarifies these problems, one should study the model for wash load prediction by combining the knowledge of these together.

From such a point of view, the production regions associated with wash load are discussed first on the basis of field data, and it is found out that the main production regions are both bare slopes and erodible banks. Secondly, mechanisms of the yield and transport of wash load are considered with the theoretical backgrounds and a new idea introduced here. According to the results, the yield and transport of wash load are predominantly subjected to gully erosion at bare slopes and bank erosion and exchange velocity between flowing water and the pore water in exchange layer. The theoretical results are supported by the data obtained from experiments. Thirdly, the authors show how the flow discharge can be evaluated in bare slopes and stream channels, and then propose a model to predict wash load concentration. If some geophysical and hydrologic parameters were given, the concentration of wash load could be calculated from the model at any time and stream section. The model has been applied to Kawarabi River Basin to test its applicability. It was found that the concentration curves predicted by the method supported the data well.

1. Introduction

Suspended sediments transported during a flood from upstream reaches are composed of particles of various sizes. Some parts of these sediments may be deposited onto the beds of natural lakes, man-made reservoirs and enlarged channel sections due to the decrease of transport capacity of flowing water there. The other parts of which particle sizes are very small will be kept in suspension for a long time in spite of the fact that the transport capacity is reduced at enlarged sections, and flowing out from reservoirs for a long duration.

According to the results of field observations reported up to this time, it is considered that most suspended sediments are composed of wash load materials. In addition, the composition rate of wash load in total load has been thought to have a high value. In some river basins of United States, it is estimated more than eighty

percent of total load. While in mountainous river basins of Japan, we have estimated it to be about fifty percent of total load.

The process of transportation of suspended sediments causes various problems associated with reservoir sedimentation, water pollution such as turbid water and so on. In order to deal with the sediment problems concerning the wash load from the point of view of hydraulic engineering, its quantitative prediction will be necessary. This study concerns the prediction of wash load concentration during a runoff due to a rain fall event.

Hitherto, many empirical methods for computing sediment graphs have been presented. Rendon[1] (1974) proposed a model which is based on an instantaneous sediment graph. But the usefulness of his method might be less universal because the method could not be applied to ungauged river basins. There are several models invented by the same way as his method. But, all of them might be thought to be less universal, because they need many data beforehand in their applications.

Mathematical and physical methods, by which the rate of wash load could be predicted at ungauged basins, have long been expected. Muramoto, Michiue and Shimojima[2] (1973) proposed a model to predict the wash load during a flood. Their model was composed of both an erosion model on bare slopes and a runoff model called "kinematic wave runoff model". Lateral inflowing water rate in unit time and channel length could be computed with the use of a runoff model. The lateral inflow of wash load was given as $W_s=p_f A_b q_s/A_d$; in which q_s is the total sediment load calculated by Brown's formula, A_b area of bare slopes formed in A_d, A_d land area of unit drainage basin (see **Fig. 19**) and p_f is the wash load composition in materials of bare slopes. Their method is more universal than the empirical methods mentioned above from the physical point of view. The model's outstanding feature may be the fact that time changes of the wash load concentration could be predicted along reaches in a drainage basin under consideration. But the model has some unpreferable properties as could be seen in the sediment transport model for the calculation of W_s in which q_s is not calculated by sheet flow discharge flowing on bare slopes but by lateral inflow discharge to stream channel. Besides, the applicability of Brown's formula is limited to noncohesive materials in most cases.

Williams[3] (1978) developed a sediment graph model based on an instantaneous unit sediment graph. The sediment graphs are predicted by convolving source runoff with an instantaneous unit sediment graph. Therefore, this method could be used on ungaged watersheds if the runoff would be known for a given rainfall. However, the change of wash load concentration could be predicted only at one section because of the use of the same runoff model as Sherman's unit hydrograph.

The hydraulic model for predicting wash load concentration presented here is developed, based on knowledge of models for stream bank and slope erosions and a runoff model called kinematic wave runoff method. The contents of the paper are as follows: Where are the production areas of wash load? What is the

mechanics of erosion in the production areas? How can we evaluate the distribution of discharge for a given rainfall in a drainage basin? These three problems will be discussed and brought together. Consequently, the mathematical and physical model for wash load is proposed, and then its applicability is shown.

2. Particle size and Source Area of Wash Load

2.1 Particle Size of Wash Load

A particle under action of flowing water takes either a state of repose or a movement in accordance with the degree of fluid force to the resistant force of the particle. Its moving state, which is classified as either suspension or traction such as rolling, sliding and saltating, could be determined by the critical shear velocities u_{*s} and u_{*c}: u_{*c} corresponds to the threshold condition of contact load and u_{*s} to that of suspension, respectively. Generally, u_{*c} can be predicted by Shields' diagram and u_{*s} may be considered nearly equal to free fall velocity ω_0 which can be calculated from Rubey's formula. In **Fig. 1**, the critical shear velocities calculated from Shields' and Rubey's formulas are shown. Referring to the curves, one could say that the particles whose critical shear velocity u_{*s} is larger than u_{*c} would behave as follows:

rest $\rightleftarrows$ contact load $\rightleftarrows$ suspending load,

with increase or decrease of fluid shear velocity. On the other hand, the particles whose u_{*s} are smaller than u_{*c} would undergo the following process:

rest $\rightleftarrows$ suspending state.

The particles which belong to the later process are thought to be washed far away from their originating or eroding area because they are transported at the same velocity as the fluid which bears them. Therefore, the particle of which critical shear velocity u_{*s} for suspension is equal to u_{*c} for contact load may be considered to have a relation with the maximum limit of particle size of wash load. Although, the particle diameter d_c with $u_{*s}=u_{*c}$ changes due to the particle density and fluid property, it could be estimated to be around 100 μm in diameter.

In order to compare the critical diameter d_c with the upper limit size of wash load, we have checked the particle sizes of wash load investigated by many investigators. The results are shown in **Table 1**, where d_{max} is the maximum diameter of wash load. Data obtained by Einstein, Anderson and Johnson[4] (1940), Einstein and Ning Chien[5] (1953), Muramoto, Michiue and

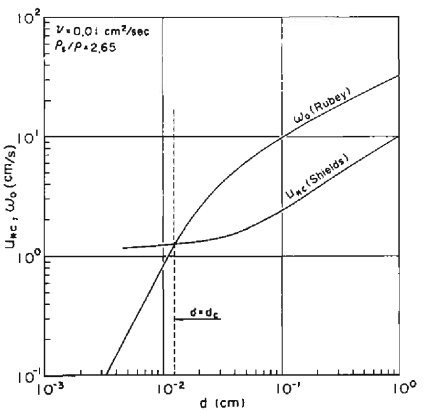

Fig. 1 Critical shear velocity and falling velocity vs. particle diameter.

Table 1 Particle size of wash load.

Investigators	Maximum diameter d_{max} (mm)	Notation
Einstein·Anderson·Johnson	0.351	Enoree River
Heidel	0.062	Bighorn River
Einstein·Ning Chien	0.06～0.1	Experimental Flume
Muramoto·Michiue·Shimojima	0.2	Daido River
Rendon-Herrero	0.1	Bixler Run Watershed
Jansen et al.	0.05～0.07	
Kanayashiki·Ashida·Egashira	0.1	Totsu River

Shimojima[2] (1973) and Kanayashiki, Ashida and Egashira[6] (1980) were decided by comparing the particle size of suspended sediment with that of bed material. The diameters of Heidel[7] (1956) and Rendon[1] (1974) were inferred from their data by the authors.

When one compares d_c with the data shown in **Table 1**, it is found that the particles finer than d_c behave as wash load in mountainous streams in most cases. Moreover, only a small amount of the particles larger than d_c might be found in suspended sediments. Therefore, it is enough for us to deal with wash load in engineering sense, concentrating on sediments finer than the critical size d_c. We define these sediments as "fine sediments" or "fine materials", although the meaning may be somewhat different from the definition in soil science. Hereafter, we will discuss the problems associated with them.

2.2 The Production Regions of Fine Sediments

Where are the fine sediments transported from? It may be considered from many field investigations that their eroding regions are stream channels and bare slopes in a mountanous drainage basin. The regions could be classified into three groups according to the differences of eroding mechanism there:

$$\text{The production regions} \begin{cases} \text{(a)} & \text{bare slope} \\ \text{(b)} & \text{erodible bank of stream channel} \\ \text{(c)} & \text{stream bed} \end{cases}$$

Here, bare slopes formed by natural forces, human activities, unpaved roads to reach forested and cultivated lands could be classified conveniently under (a). Banked sediments and debris, land slide regions and man made sediments along the river banks are classified under (b). The region (c) is defined as the stream part where the bed sediments are within the flowing water in the usual state without flood duration.

On the bare slopes, the sediment yield and transport can only occur during surface runoff due to rainfall, or the runoff formed by snow melting. On the other hand, the sediment yield starts in the region (b) by bank erosion which occurs over

a critical discharge in a stream channel. In the channel bed, the sediments transported from upstream reach and those existing at the critical area are transported as both are exchanged each other. If the fine sediments exist in each region in significant quantities, they are washed out as wash load from their original regions. Egashira and Ashida[8] (1981) carried out the field investigation for the composition rate of fine sediments at various river basins, and found that it was 10–20% in materials of region (a) and around 2% in region (c), and in region (b) the composition rate was between the two.

It is valuable to discuss regions from which the fine sediments might be originated. This problem is discussed on the basis of field data. Denoting that discharge of the fine sediments is V_f in unit time and area at a given section of a river basin, V_f is formulated as

$$V_f = V_{fs} + V_{ft} + V_{fb} \qquad \cdots\cdots(1)$$

in which V_{fs} is the discharge of fine sediments from bare slopes, V_{ft} from stream banks or terraces and V_{fb} from beds.

The third term on the right hand side of eq. (1) has been neglected empirically:

$$V_{fb} \doteqdot 0 \qquad \cdots\cdots(2)$$

It seems to be somewhat dangerous to accept eq. (2) without proof, because the quantities of fine sediments from bed regions may not be negligible due to the area being more extensive than any other region, although composition rate of fine sediments is negligibly small. Therefore, let us ascertain the truth of eq. (2), referring to the change of composition rate of fine sediments in bed materials sampled at the same places before and after a flood. The field investigation was carried out at the Kawarabi river (see **Fig. 20**). The sampling method was as follows: Twelve points of channel bed near flowing water surface along the reach were chosen as the sampling stations. The materials were sampled there before a flood and then a tracer as much as the quantity of the sampled materials was buried instead. When a flood occurred, the tracer from bed surface to some depth was washed out due to the bed variation. Sediments were deposited, replacing the tracer after the flood. Then the deposited materials were sampled at each station.

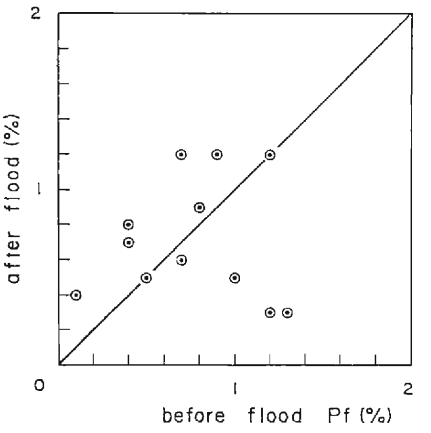

Fig. 2 Composition rate of fine sediments in bed materials before and after flood.

Fig. 2 shows the results concerning the composition rate of fine sediments in materials sampled before and after a flood. As is seen in the figure, no systematic

changes in the rate of fine sediments are recognizable. Some data show increases and some others show decreases in the fine sediment rate after the flood. Consequently, it may be inferred from the results that the outflowing discharge of fine sediments would be negligibly small. Therefore, eq. (2) can be accepted at the present time in most drinage basins of Japan.

From the fact mentioned above, eq. (1) is reduced to

$$V_f = V_{fs} + V_{ft} \qquad \cdots\cdots(3)$$

In the previous treatments on problems of wash load, much attention has been paid to the first term V_{fs} in most cases, and rather less to the second term V_{ft}. The following consideration concerns V_{fs} and V_{ft}. Denoting that area of a drainage basin is A_d, area of bare slopes formed in the basin A_b, the height of erodible bank D, the total length of erodible bank l_t, stream length l, eroding depth in unit time at bare slopes and erodible banks d_{se} and d_{te} respectively, eq. (3) is transformed into

$$A_d V_f = (1-\lambda_{bs}) p_{fs} A_b d_{se} + (1-\lambda_t) p_{ft} f_t l D d_{te} \qquad \cdots\cdots(4)$$

in which $f_t = l_t/l$ $(0 \leq f_t \leq 1)$, λ_{bs} and λ_t are porosities of bare slopes and erodible banks respectively, p_{fs} the composition rate of fine sediments in materials eroded at bare slopes, and p_{ft} that in materials eroded at stream banks. Comparing eq. (3) with (4) gives

$$V_{fs} = (1-\lambda_{bs}) p_{fs} d_{se} A_b / A_d \quad \text{and} \quad V_{ft} = (1-\lambda_t) p_{ft} f_t l D d_{te} / A_d.$$

It may be considered that the area of erodible banks is large where the drainage basin possesses many bare slopes. The following relation, therefore, is deduced:

$$dV_{ft}/dV_{fs} > 0 \quad \text{or} \quad d(f_t l D)/dA_b > 0 \qquad \cdots\cdots(5A)$$

The most simple formula of eq. (5A) may be

$$f_t l D \propto A_b \qquad \cdots\cdots(5B)$$

Substituting eq. (5A) or (5B) into eq. (4) gives the functional relation:

$$A_d V_f = F_b(A_b) = F_t(f_t l) \qquad \cdots\cdots(6)$$

in which F_b and F_t are functional descriptions, respectively. Eq. (6) means that the discharge of fine sediments depends on both the area of bare slopes and that of erodible banks and moreover it could be described with either of the two if eq. (5A) holds.

It should be examined whether the formula is relevant or not with use of field data. The discharges of fine sediments versus the area of bare slopes are shown in **Fig. 3**, and those versus the lengths of erodible banks in **Fig. 4**, respectively. The data used here were obtained at several measuring stations in the Kawarabi river basin (see **Fig. 20**) during two floods which occurred in June, 1979. As shown on these figures, one will be able to see the clear relations between the discharge of fine sediments and both A_b and $f_t l$. These macroscopic discussions associated with

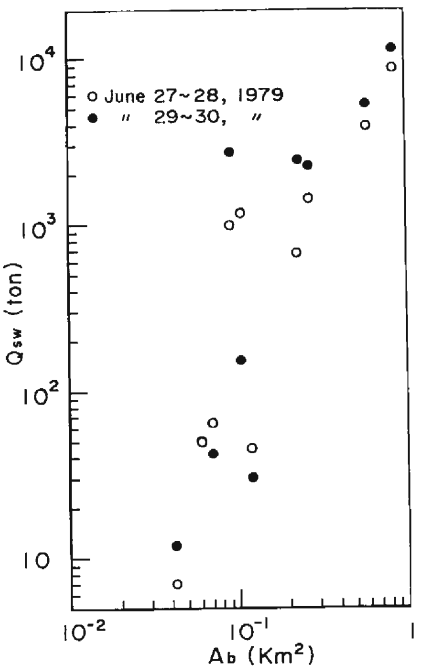

Fig. 3 The accumulated mass of fine sediments washed out during two runoffs occurred on June in 1979 vs. the area of bare slopes in the Kawarabi river basin.

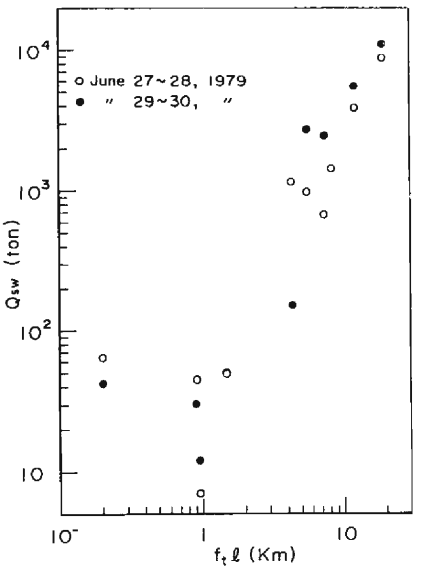

Fig. 4 The accumulated mass of fine sediments washed out during two runoffs occurring on June in 1979 vs. the lengths of erodible banks in the Kawarabi river basin.

the production regions of fine sediments say that they should be yielded and transported from the regions of bare slopes and erodible banks upstream. In other words, their production regions are as follows:

$$\text{The production regions} \begin{cases} \text{(A)} & \text{bare slopes} \\ \text{(B)} & \text{erodible banks} \end{cases}$$

3. The Yield and Transport of Fine Sediments at Bare Slopes

3.1 The Threshold of the Movement of a Coarse Grain in Cohesive Materials and Its Eroding Process

Generally, it is the fact that the materials of bare slopes contain some quantities of fine sediments as described in Chap. 2. Materials composed of fine sediments exhibit a little resistance to an external force due to their cohesion, in addition to the gravitational and frictional forces. Therefore, the threshold condition of particles in cohesive materials may be different from that of noncohesive materials.

For simplicity, it is supposed that the slope under consideration would be composed of the fine sediments and uniform coarse materials. A part of cross

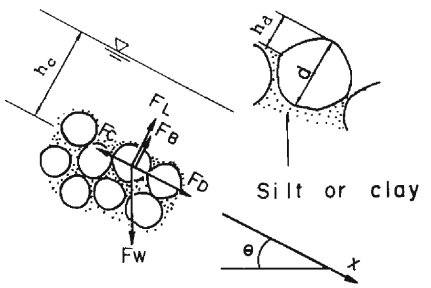

Fig. 5 Forces acting on a coarse particle within cohesive materials.

sectional view of the slope is shown in **Fig. 5**, and resistant and fluid forces also shown schematically there. The equilibrium state of these forces under the threshold in movement of the coarse material results in

$$F_D+F_w\sin\theta=F_c+(F_w\cos\theta-F_L-F_B)\tan\varphi \quad\cdots\cdots(7)$$

in which θ is the inclination angle of the slope, F_w gravitational force acting on the coarse particle, F_B buoyancy force, F_D drag force, F_L lift force, F_c cohesive force and φ angle of repose of the coarse material. The following descriptions are given to these forces:

$$F_D=1/2\cdot\rho C_D k_1 d^2 u_d^2 \quad\cdots\cdots(8)$$

$$F_L=1/2\cdot\rho C_L k_2 d^2 u_d^2 \quad\cdots\cdots(9)$$

$$F_w=\rho_s k_3 d^3 g \quad\cdots\cdots(10)$$

$$F_B=\rho k_3 d^3 g\cos\theta \quad\cdots\cdots(11)$$

$$F_c=k_1' d^2 f_c \quad\cdots\cdots(12)$$

where, C_D is the coefficient of drag force, C_L the coefficient of lift force, d the particle diameter of coarse material, ρ_s particle density, ρ fluid density, u_d velocity acting on the particle, k_1, k_2 and k_1' correction factors of projected surface area of the particle, and f_c cohesive force in unit surface area resisting the fluid force. Substituting eqs. (8), (9), (10), (11) and (12) into eq. (7) and then putting $u_d=au_*$ give

$$\tau_{*cc}\equiv\frac{u^2_{*cc}}{(\rho_s/\rho-1)gd}=\frac{2k_3}{C_D(k_1+k_2C_L/C_D\cdot\tan\varphi)}\frac{1}{a^2}\left(\cos\theta\tan\varphi-\frac{\rho_s}{\rho_s-\rho}\sin\theta\right)+\frac{2k_1'}{C_D(k_1+k_2C_L/C_D\cdot\tan\varphi)}\frac{1}{a^2}\frac{f_c}{(\rho_s-\rho)gd} \quad\cdots\cdots(13)$$

in which τ_{*cc} is non-dimensional drag stress in threshold condition and u_{*cc} critical shear velocity. From the analogy to non-dimensional shear stress, non-dimensional cohesive stress is defined by

$$f_{c*}=f_c/(\rho_s-\rho)gd \quad\cdots\cdots(14)$$

Using Shields' parameter τ_{*c} developed for mild slope and f_{c*} defined by eq. (14), eq. (13) is reduced to

$$\tau_{*cc}=\left(\cos\theta\tan\varphi-\frac{\rho_s}{\rho_s-\rho}\sin\theta\right)\frac{\tau_{*c}}{\tan\varphi}+\frac{k_1'\tau_{*c}}{k_3\tan\varphi}f_{c*} \quad\cdots\cdots(15)$$

In eq. (15), τ_{*cc} becomes equal to Shields' parameter τ_{*c} in the case that f_{c*} and θ are negligibly small. The second term of eq. (15) involving f_{c*} represents the effect of cohesion due to fine sediments on critical tractive stress of the coarse particle.

One can find that coarser materials exist in statically stable states even on the steep slope of angle θ larger than the angle of repose φ. This is the reason why the fine sediment exerts a resistance force on the particle.

Unfortunately, it may be impossible to evaluate the cohesive stress associated with physical and chemical properties of fine sediments. However, it is possible to discuss the erosion and transportation of the cohesive materials under a given condition. For example, the erosion process of cohesive materials could be discussed experimentally. Ashida and Sawai[9] (1976) discussed the eroding velocity of a stream bed composed of coarse materials and fine sediments such as bentnite. They determined the following relation:

$$E_*=E/u_*=\text{const.} \qquad \cdots\cdots(16)$$

in which E is the erosion velocity, E_* its non-dimensional one and u_* the shear velocity on a bed. In eq. (16), E_* is a constant which depends on the soil properties. Eq. (16) has been applied to the soil which has a uniform erodibility.

Now then, we will look at the erosion process of a soil layer. Concentrating our eyes on the surface of soil layer with a uniform erodibility at a fixed point in an eroding event, we could see its eroding process in **Fig. 6(a)**. In this figure, h_d/d is the non-dimensional depth of fine sediments from the top of coarse particle to the surface of fine sediments (see **Fig. 5**), τ_* non-dimensional shear stress of fluid flow, τ_{*r} the resistant stress of soil surface, T periodic time of the coarse particle detachment, T' time necessary from one detachment to the next detachment and $\bar{T}=T-T'$. Putting τ_* instead of τ_{*c} in eq. (15), we get the formula of resistant stress τ_{*r} instead of τ_{*cc}. From the resultant equation, it is understood that the resistant stress changes with k_1' which is a function of h_d/d. With the progress of detachment of fine sediment, k_1' would take a lower value because of increase of h_d/d. Therefore, τ_{*r} exhibits a cyclic change in accordance with the change of h_d/d. τ_{*r} has a minimum degree τ_{*rmin} just before the detachment of a coarse particle. In case that $\tau_*>\tau_{*rmin}$, the eroding process is shown as in **Fig. 6(a)**. We define such a process as "*the erosion process of weak layer*". If $\tau_{*rmin}>\tau_*$, the erosion of soil layer would have to cease. In the case that the fine sediments are eroded to a certain

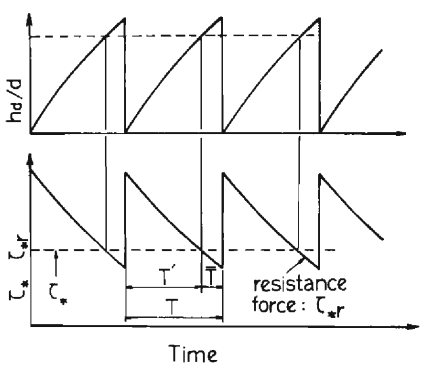

Fig. 6(a) Erosion process of "weak soil layer".

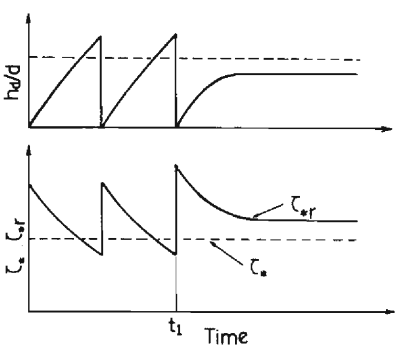

Fig. 6(b) Erosion process of "strong soil layer".

maximum depth due to the low erodibility of soil or the sheltering effect of a coarse particle, the particle can not be detached. Therefore the erosion of soil ceases and then an armour coat is formed over the surface layer of soil. An erosion process with armouring phenomena is shown in **Fig. 6(b)**. A weak soil layer is eroded till the time t_1 when the low erodibility soil surface appears. After that time, the soil layer can not be eroded any deeper than the diameter of a coarse particle. We define such a process as "*the erosion process of strong layer*".

3.2 Sediment Yield and Transport Due to Gully Erosion

(1) Formulation of Sediment Yield and Transport

Consider that a bare slope is composed of two soil layers: a weak soil layer which is $\alpha_1 d$ in depth. It is underlain by a strong layer. It undergoes erosion process as shown in **Fig. 6(b)**. We suppose that the upper layer possesses the erosion velocity E_1, porosity λ_1, composition rate of fine sediments p_{f1} and that of coarse materials p_{c1}, and those of the lower layer are E_2, λ_2, p_{f2} and p_{c2}, respectively. Moreover, the erosion process of the weak layer takes place until the eroded depth becomes $\alpha_1 d$; and then that of strong layer continues until the armouring phenomena are finished.

Under these condition, sediment yield in unit time and area is given as:

$$m_t=\rho_s E_1(1-\lambda_1)(p_{f1}+p_{c1}),\ (p_{f1}+p_{c1}=1)$$

This foumula is shown schematically in **Fig. 7**. In regard to the yield of fine sediments, one obtains

$$m_f=\rho_s E_1(1-\lambda_1)p_{f1},\ (t\leq t_1) \qquad \cdots\cdots(16)$$

in which t_1 is the time when the erosion of the weak layer is finished.

$$t_1=\alpha_1 d/E_1 \qquad \cdots\cdots(17)$$

On the other hand, the total amount of fine sediments produced in the erosion process of the strong layer can be described by

$$\rho_s \alpha_2 d(1-\lambda_2)p_{f2}$$

in which $\alpha_2 d(\alpha_2<1)$ is the depth erodible in the erosion process of the strong layer. Noting that the quantity of fine sediments having been eroded between t_1 and denotes M_{out} and that of fine sediments remained in the bed M_b, one obtains

$$M_{out}+M_b=\rho_s \alpha_2 d(1-\lambda_2)p_{f2}=\text{const.} \qquad \cdots\cdots(18)$$

and then

$$dM_{out}/dt=-dM_b/dt \qquad \cdots\cdots(19)$$

The porosity λ and the composition rate p_f of fine sediments in the layer $\alpha_2 d$ change in accordance with the progress of an erosion process. Therefore, dM_{out}/dt and dM_b/dt are written as follows:

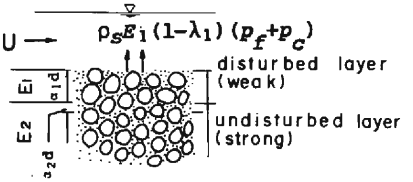

Fig. 7 Schematic diagram of the yield of fine sediments.

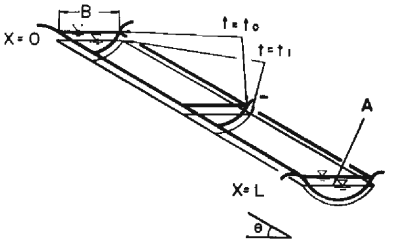

Fig. 8 Sketch of erosion process within a single gully.

$$dM_{out}/dt=\rho_s E_2\{1-\lambda(t)\}p_f(t) \qquad \cdots\cdots(20)$$

$$dM_b/dt=\rho_2 a_2 d\frac{d}{dt}[\{1-\lambda(t)\}p_f(t)] \qquad \cdots\cdots(21)$$

From eqs. (19), (20) and (21), the following formula is obtained.

$$\{1-\lambda(t)\}p_f(t)=(1-\lambda_2)p_{f2}\exp[-E_2(t-t_1)/a_2 d] \qquad \cdots\cdots(22)$$

Substituting eq. (22) into (20) gives the relation for the yield of fine sediments in unit time and area:

$$m_f=\rho_s(1-\lambda_2)p_{f2}E_2\exp[-E_2(t-t_1)/a_2 d],\ (t_1<t) \qquad \cdots\cdots(23)$$

Fig. 8 shows the sketch of a gully which possesses L in length, A in area of flow section, B in flow width and θ in inclination slope angle. The concentration of fine sediments due to gully erosion is described by

$$\frac{\partial c}{\partial t}+\frac{Q}{A}\frac{\partial c}{\partial x}=\frac{1}{\rho}\frac{S_p}{A}m_f \qquad \cdots\cdots(24)$$

in which c is the concentration of fine sediments, S_p the length of wetted perimeter, $S_p/A=R$, Q flow discharge, and m_f is represented by eq. (16) or (23). In case of constant discharge, the above equation can be solved analytically.

$0\leq t\leq t_1$ (in case of erosion process of weak layer)

$$c(x)=\frac{\rho_s}{\rho}(1-\lambda_1)E_{1*}u_*p_{f1}\frac{x}{UR} \qquad \cdots\cdots(25A)$$

$t_1<t$ (in case of erosion process of strong layer)

$$c(t,x)=\frac{\rho_s}{\rho}(1-\lambda_2)p_{f2}\frac{a_2 d}{R}(\exp[E_{2*}u_*/a_2 dU]-1)\cdot\exp[-E_{2*}u_*(t-t_1)/a_2 d] \qquad \cdots\cdots(25B)$$

In eqs. (25A) and (25B), $U=Q/A$, E_{1*} and E_{2*} are defined as follows:

$$E_{1*}=E_1/u_* \qquad \cdots\cdots(26A)$$

$$E_{2*}=E_2/u_* \qquad \cdots\cdots(26B)$$

where E_{1*} and E_{2*} are supposed to be constants which should be decided empirically.

(2) Discussion on the Sediment Transport Formulas and the Results of Field Experiments

For applications of eqs. (25A) and (25B) to some practical problems, E_{1*}, E_{2*}, velocity factor U/u_* and some unknown factors contained in these equations should be given previously. Therefore, field experiments were carried out to do so. Four bare slopes were chosen in the Akadani river basin which is a tributary of the Kawarabi river basin (see **Fig. 20**), and three or five gullies which are trapezoid in cross section and 150~716 m in length were made on each slope. Then, some hydraulic quantities relating to the gully erosion were investigated in each gully by several measurements such as discharge, flow velocity, channel geometry, concentration of fine sediments in flowing water and so on. Experimental equipment and methods have been reported already by Ashida, Egashira and Kanayashiki[10] (1980). Therefore, only the results are shown below.

Fig. 9 shows the relation obtained from the field experiments between flow discharge and width of flowing water surface. From the figure, it is found that Lacy's regime formula might hold, so the width could be written as

$$B=\alpha' Q^{1/2} \quad (\alpha'=5;\ m\text{-sec unit}) \qquad \cdots\cdots(27)$$

in which B is the width and Q discharge of flowing water.

Fig. 10 shows the friction factor defined by Darcy-Weisbach. In **Fig. 10**, empirical curves from Ashida, Daido, Takahashi and Mizuyama[11] (1973) are also indicated in order to compare data obtained from experiments with their curves. Although data plotted might be predicted by their curves with parameter u_*^2/gd_m in which d_m is the mean diameter of coarse grains, these data are plotted outside of their application limit unfortunately. However, the logarithmic law could be applied to these data in a crude sense.

Fig. 11 shows the relation between $E_1/u_*(=E_{1*})$ and shear stress acting on a

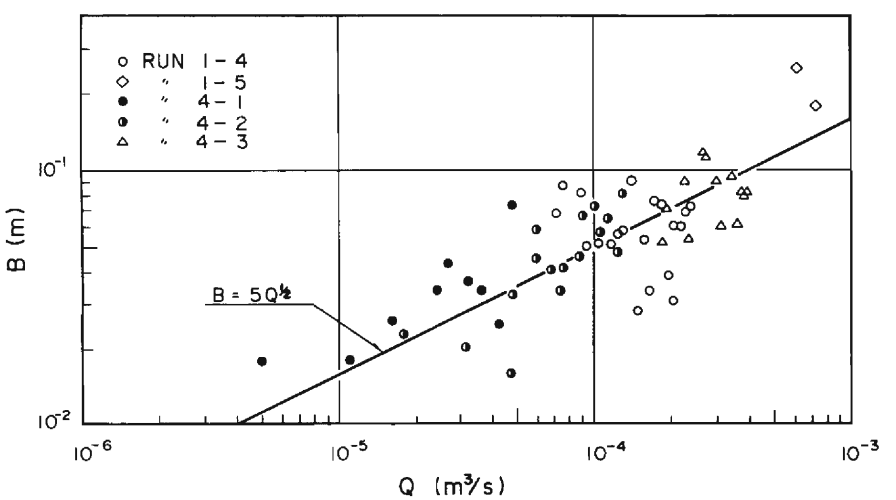

Fig. 9 Width of flowing water surface vs. flow discharge.

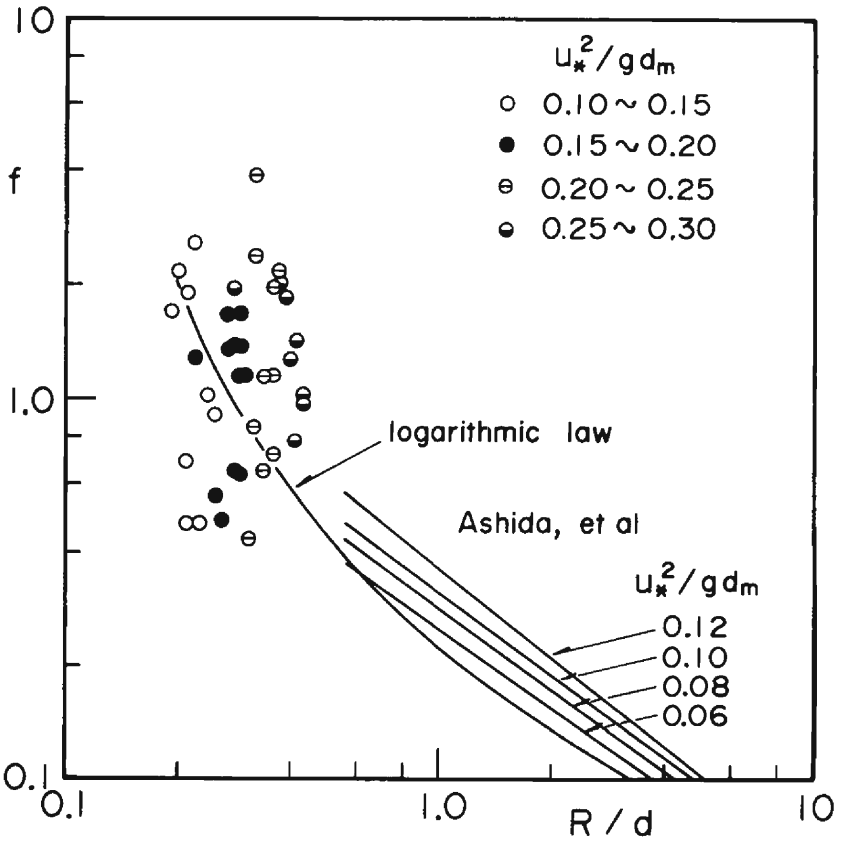

Fig. 10 Friction factors in gully flows.

bed surface. The data of the same Run No. belong to the same bare slope: The data numbered Run 1–1~1–5 were obtained at the bare slope labeled 1. These data may be scattered somewhat as seen in **Fig. 10**, because the accuracy of experiment was not complete due to the field experiments. However, the data obtained from Run 1–1~Run 1–5 indicate that eq. (26A) holds.

The results mentioned above and some hydraulic variables necessary for the application of eq. (25A, B) have been obtained from field experiment and an additional investigation. Now, we will test the applicability of eqs. (25A) and (25B) with use of these data. The fine sediment concentration in flowing water at the downstream end of a gully can be obtained from these two equations by substituting the gully length into x.

In **Figs. 12(a)** and **(b)**, the time changes of the concentration washed out from the gullies are shown in the case where the erosion process of the weak layer occurs first and then that of a strong layer follows. In **Figs. 13(a)** and **(b)**, the case where only the erosion process of the strong layer occurs is shown. On the figures, the full lines are obtained from eqs. (25A) and 25(B) with use of paramenters tabulated in **Table 2.**

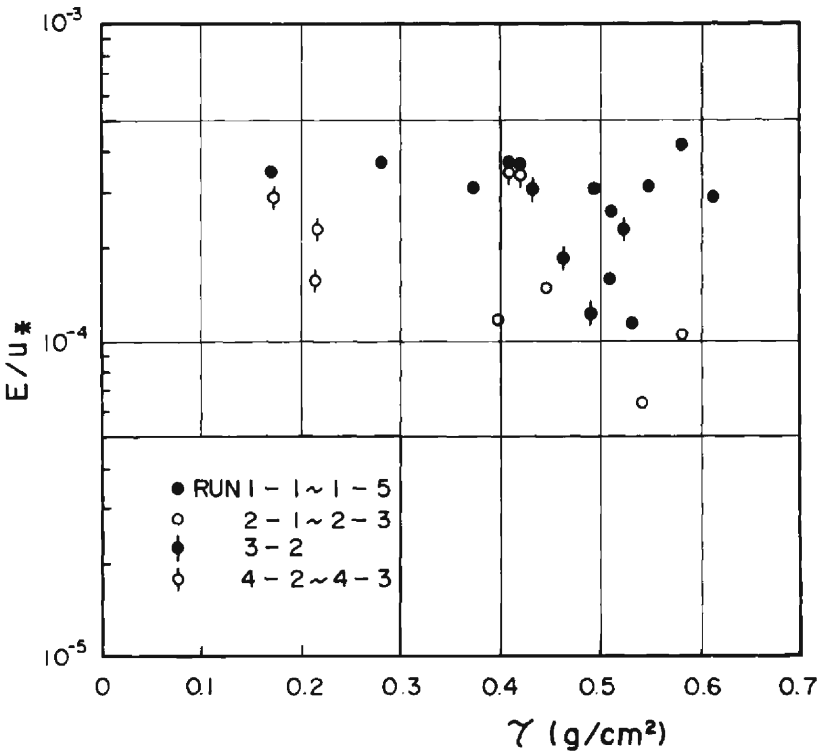

Fig. 11 Nondimensional erosion velocities in the process of weak soil layers.

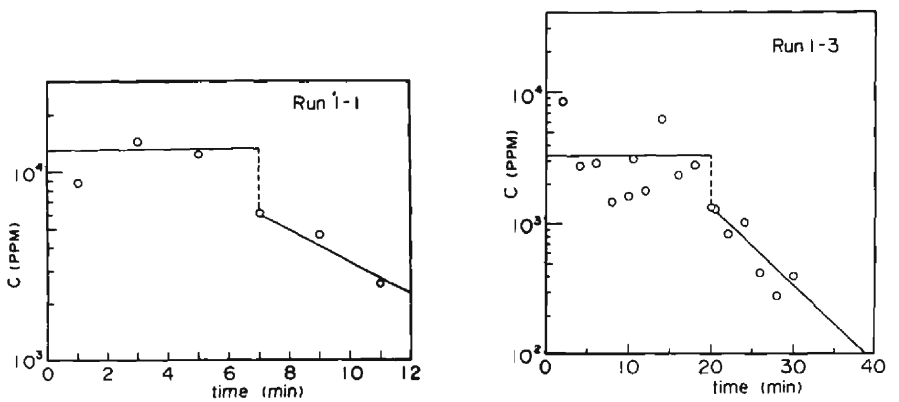

(a) (b)

Fig. 12(a), (b) Comparisons between theory and experiment with respect to the fine sediment concentrations at the downstream end of gullies in the case that erosion process of weak soil layer occurs first and then that of strong soil layer occurs.

Table 2 Parameters used for the calculation.

Run No.	10^4E_{1*}	10^4E_{2*}	α_1	α_2	d_m(cm)	$p_{f1}(=p_{f2})$	$\lambda_1(=\lambda_2)$	U (cm/s)	R (cm)
1 - 1	3.58	1.98	1.51	0.62	1.95	0.08	0.4	51.5	0.600
1 - 3	0.74	0.55	0.96	0.26	1.95	0.08	0.4	60.5	0.699
2 - 3	—	1.29	0	0.71	1.94	0.08	0.4	55.3	0.678
4 - 3	—	0.71	0	0.49	0.86	0.15	0.4	57.1	0.491

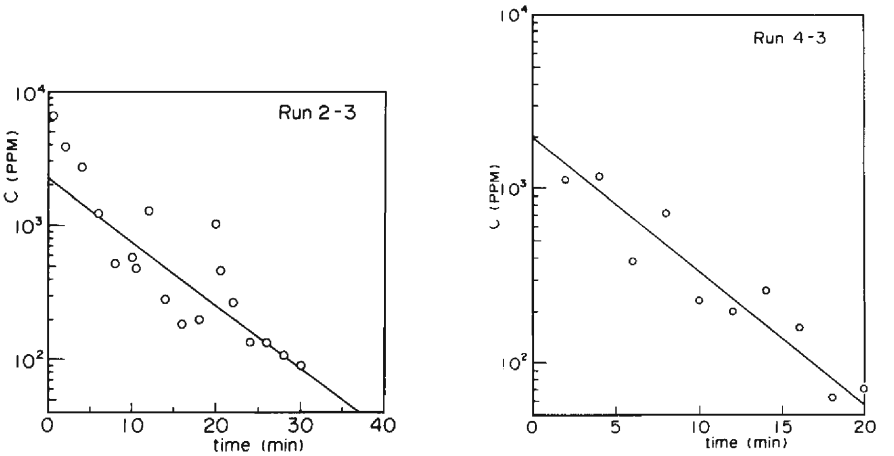

(a) (b)

Fig. 13(a), (b) The comparisons between theory and experiment with respect to the fine sediment concentrations at the downstream end of gullies in the case that only erosion process of strong soil layer occurs.

From the comparisons shown in **Figs. 12(a) (b)** and **Figs. 13(a) (b)**, it is found that the data are scattered a little around the lines predicted by eq. (25A) for the process of weak soil layer and by eq. (25B) for that of the strong layer. The scattering might be caused by the geometric irregularity of the gully surface in the degree of coarse particle size. This scattering exhibits no trends. Therefore, the concentration of fine sediments from gully erosion could be predicted well enough by eqs. (25A) and (25B).

4. The Yield and Transport of Fine Sediments in Stream Channels

4.1 The Mechanism of Sediment Yield and Transport

As discussed by Ashida, Egashira, Kanayashiki and Ogawa[12] (1980), yield mechanisms of fine sediments can be classified into three groups: (1) The yield from bank and bed erosion; (2) The trap by deposition of coarse grains; (3) The yield or trap by the mixing action between flowing water and the pore water in sediments and debris.

The yield of fine sediments by the first mechanism is described as follows.

$$M_{1s}=\rho_s p_{fs} q_s \qquad \cdots\cdots(28)$$

$$M_{1b}=-\rho_s p_{fb}(1-\lambda_b) B\partial Z/\partial t,\ (\partial Z/\partial t<0) \qquad \cdots\cdots(29)$$

in which M_{1s} is the yield quantity of fine sediments in unit time and length due to bank erosion, p_{fs} composition rate of fine sediments of bank materials, q_s bank erosion rate in absolute volume, M_{1b} the yield from the bed due to bed erosion, p_{fb} composition rate of fine sediments of bed materials, λ_b porosity of bed materials and B the channel width, where the cross section is supposed to be rectangular for simplicity. q_s is written by

$$q_s=(1-\lambda_s) D\partial B/\partial t \qquad \cdots\cdots(30)$$

in which λ_s is porocity of bank materials and D the height of stream bank. Moreover, the fine sediments suspended in the pore water of bank and bed materials are washed out, and then the yields are described by

$$M_{1ss}=\rho c_s e_s q_s,\ (e_s=\lambda_s/(1-\lambda_s)) \qquad \cdots\cdots(31)$$

$$M_{1bs}=-\rho c_b \lambda_b B\partial Z/\partial t \qquad \cdots\cdots(32)$$

in which c_s and c_b are concentrations of fine sediments in pore water of bank and bed materials, respectively. The yield of fine sediments by the second mechanism is described by

$$M_{bt}=-\rho c\lambda_b B\partial Z/\partial t \qquad \cdots\cdots(33)$$

in which c is the concentration of fine sediments in stream water. Those by the third one can be written with use of exchange velocity introduced by Ashida, Egashira, Kanayashiki and Ogawa (1980).

$$M_{se}=2\rho V_{es}(c_s-c)\lambda_s h \qquad \cdots\cdots(34)$$

$$M_{be}=\rho V_{eb}(c_b-c)\lambda_b B \qquad \cdots\cdots(35)$$

in which V_{es} and V_{eb} are the exchange velocities at bank and bed surfaces, and h water depth.

Combining these equations, one gets

$$\frac{\partial}{\partial t}(\rho cA)+\frac{\partial}{\partial x}(\rho cQ)=(\rho_s p_{fs}+\rho c_s) q_s+F(\partial Z/\partial t) +2\rho\lambda_s h(c_s-c)+\rho\lambda_b B(c_b-c) V_{eb} \qquad \cdots\cdots(36)$$

in which $F(\partial Z/\partial t)$ is a function of bed variation and other variables.

$$F(\partial Z/\partial t)=\begin{cases}-\{\rho_s(1-\lambda_b)p_{fb}+\rho c_b\lambda_b\} B\partial Z/\partial t, & (\partial Z/\partial t<0)\\ -\rho c\lambda_b B\partial Z/\partial t, & (\partial Z/\partial t\geqq 0)\end{cases}$$

Equation of continuity of water mass will be shown below. It is the fact that the pore water in bank and bed is added to the flowing water due to the erosion and deposition of materials, except the lateral inflow from the mountain slopes. Therefore, the continuity of water mass in flowing water is described by

$$\frac{\partial A}{\partial t}+\frac{\partial Q}{\partial x}=e_s q_s-\lambda_b B\frac{\partial Z}{\partial t} \qquad \cdots\cdots(37)$$

in which the lateral inflow from mountain slopes is excluded, as it will be discussed in Chap. 5. From eqs. (36) and (37), the partial differential equations for the concentration of fine sediments are obtained:

$\partial Z/\partial t<0$;

$$\frac{\partial c}{\partial t}+U\frac{\partial c}{\partial x}=\frac{1}{A}\left\{\frac{\rho_s}{\rho}p_{fs}+e_s(c_s-c)\right\}q_s+\frac{1}{A}\left\{2\lambda_s h(c_s-c)V_{es}+\lambda_b B(c_b-c)V_{eb}\right\}-\frac{B}{A}\left\{\frac{\rho_s}{\rho}(1-\lambda_b)p_{fb}+\lambda_b(c_b-c)\right\}\frac{\partial Z}{\partial t} \qquad \cdots\cdots(38)$$

$\partial Z/\partial t\geqq 0$;

$$\frac{\partial c}{\partial t}+U\frac{\partial c}{\partial x}=\frac{1}{A}\left\{\frac{\rho_s}{\rho}p_{fs}+e_s(c_s-c)\right\}q_s+\frac{1}{A}\left\{2\lambda_s h(c_s-c)V_{es}+\lambda_b B(c_b-c)V_{eb}\right\} \qquad \cdots\cdots(39)$$

in which $U=Q/A$.

According to the discussions carried out by Ashida, Egashira et al[12] (1980), the third term described by $-B/A\cdot\{\cdots\cdots\}\partial Z/\partial t$ in eq. (38) is negligibly small in general cases. Therefore, eq. (38) is reduced to eq. (39), and eq. (39) can be used in both the degrading and agrading states.

4.2 The General Formula of Transport Equation and its Application

(1) Variables in the Transport Equation

(a) Exchange Velocity

It is considered that exchange velocity is influenced by kinematic viscosity ν, shear velocity u_*, flow depth h, particle diameter d and porosity λ_b. Dimensional analysis gives

$$V_{eb}/u_*=F(u_*d/\nu,\ h/d,\ \lambda_b) \qquad \cdots\cdots(40)$$

in which F is a functional description to be determined by experiments and $V_{eb}/u_*(=V_{eb*})$ a non-dimensional exchange velocity. Ashida, Egashira et al[12] (1980) investigated its form by flume experiments. The Data are classified into three groups with relative depth h/d, and plotted in **Fig. 14**. The abscissa is the grain Reynolds number. They do not scatter so much. Besides, they do not exhibit a systematic change not only by u_*d/ν but also h/d. Consequently, non-dimensional exchange velocity could be described as

$$V_{eb}/u_*=V_{eb*}=\text{const.}\ (V_{eb*}=4.3\times10^{-3}) \qquad \cdots\cdots(41)$$

(b) Concentration of Fine Sediments in Exchange Layer

The flux of fine sediments at exchange layer is shown schematically in **Fig. 15**.

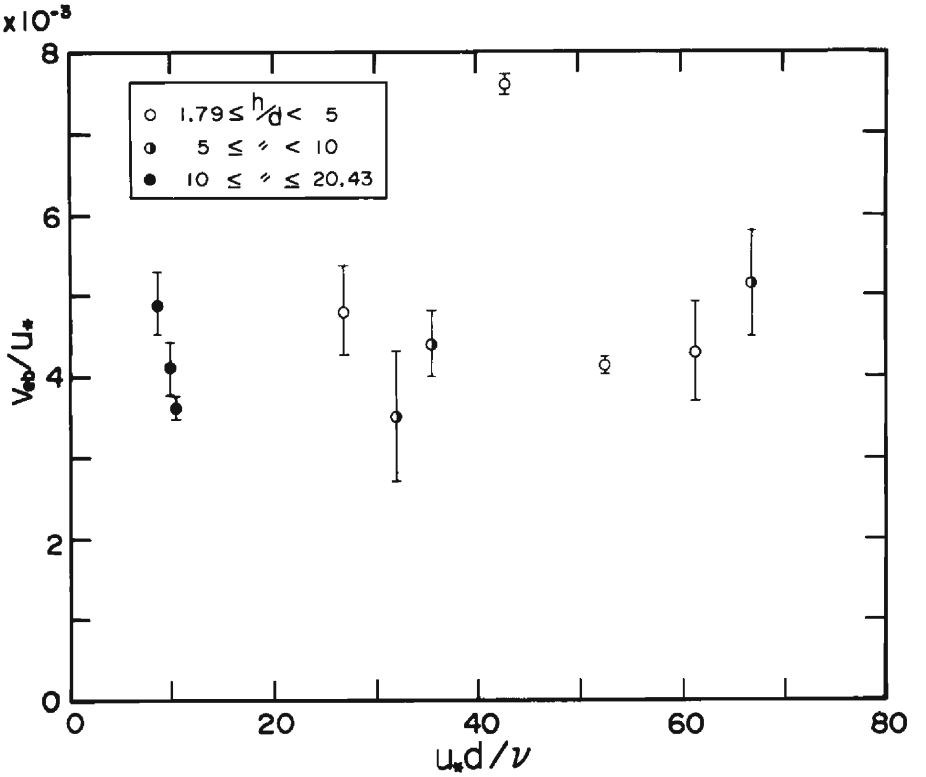

Fig. 14 Nondimensional exchange velocity.

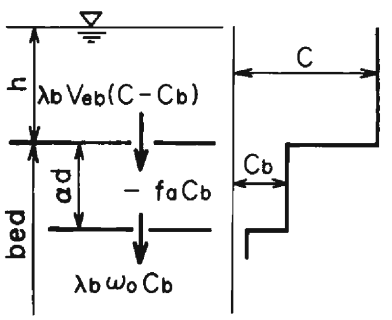

Fig. 15 Schematic diagram of the flux of fine sediments in the exchange layer.

The thickness of the layer might be estimated to be ad (a=2~3) according to the studies (e.g. Zagni[13], 1976) associated with shearing flows on permeable beds. If the concentration of flowing water is larger than that of exchange layer, fine sediments is transferred into exchange layer through the bed surface. $\lambda_b\omega_0 c_b$ of the quantity of fine sediments is transferred from the exchange layer to the lower region due to their deposition. Moreover, the fine sediments might be deposited and absorbed at the exchange layer. From these explanations, one can obtain the following formula concerning the time change of fine sediments concentration suspended in the exchange layer.

$$\frac{dc_b}{dt}=-\left(\frac{V_{eb}}{ad}+\frac{\omega_0}{ad}+\frac{f_a}{\lambda_b}\right)c_b+\frac{V_{eb}}{ad}c \qquad \cdots\cdots(42)$$

in which ω_0 is the falling velocity of fine sediments and f_a the absorbing coefficient due to deposition and absorption of fine sediments. The solution of eq. (42) under an initial condition with $c_b=0$ at $t=0$ gives

$$c_b=\frac{k_2}{k_1}c(1-e^{-k_1t}) \qquad \cdots\cdots(43)$$

in which

$$\left.\begin{aligned} k_1&=V_{eb}/ad+\omega_0/ad+f_a/\lambda_b \\ k_2&=V_{eb}/ad \end{aligned}\right\} \qquad \cdots\cdots(44)$$

Taking silt and clay sizes and eq. (41) into consideration, eq. (43) gives the steady solution

$$c_b=\frac{k_2}{k_1}c=\frac{V_{eb}}{V_{eb}+\omega_0+ad/\lambda_b\cdot f_a}c \qquad \cdots\cdots(45)$$

Consequently, c_b can be determined if f_a is known.

A brief discussion will be taken to estimate f_a. Noting N is the number of coarse grains occupied in a unit volume of exchange layer, and supposing absorption of fine sediments in the exchange layer could occur only due to their deposition onto the surface of grains there, the following relation must hold.

$$f_ac_b=A_sN\omega_0c_b \qquad \cdots\cdots(46)$$

in which $N=6(1-\lambda_b)/\pi d^3$ and $A_s=\pi/4\cdot d^2$.

Then,

$$f_a=3/2\cdot(1-\lambda_b)/\omega_0 d \qquad \cdots\cdots(47)$$

Substituting eqs. (41) and (47) into eq. (45) gives

$$c_b=1/\{1+\gamma\omega_0/u_*\}\cdot c \qquad \cdots\cdots(48)$$

in which

$$\gamma=\{1+3a(1-\lambda_b)\}/2\lambda_bV_{eb*} \qquad \cdots\cdots(49)$$

Eq. (48) can be transformed into

$$(c-c_b)/c=\chi(\omega_0/u_*) \qquad \cdots\cdots(50)$$

in which $\chi(\omega_0/u_*)$ is defined by

$$\chi(\omega_0/u_*)=\frac{\gamma\omega_0/u_*}{1+\gamma\omega_0/u_*} \qquad \cdots\cdots(51)$$

Supposing $ad=(2\sim3)d$, $\lambda_b=0.4$ and $V_{eb*}=4.3\times10^{-3}$, γ defined by eq. (49) takes values within

$$1.3\times10^3\leq\gamma\leq1.8\times10^3 \qquad \cdots\cdots(52)$$

Fig. 16 shows the relation between $\chi(\omega_0/u_*)$ and ω_0/u_*. From the results shown in the figure, it is understood that the concentration of fine sediments in the

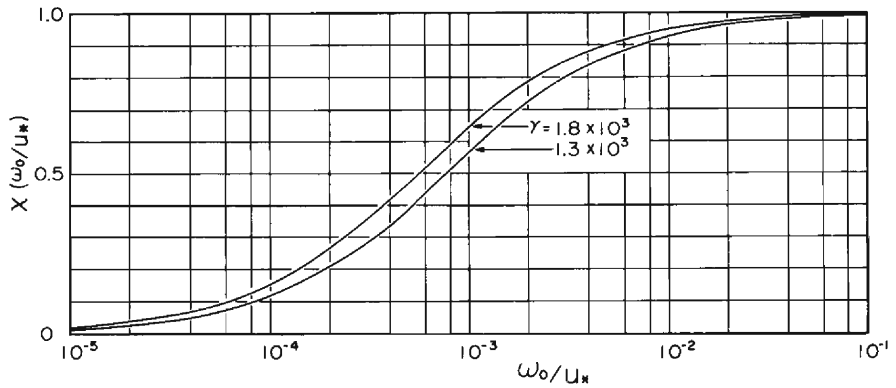

Fig. 16 $\chi(\omega_0/u_*)$ vs. ω_0/u_* (see eq. 50).

exchange layer approximates

$$c_b=0 \quad \text{at} \quad \chi(\omega_0/u_*)=1 \quad (\omega_0/u_*\to 1)$$

and

$$c_b=c \quad \text{at} \quad \chi(\omega_0/u_*)=0 \quad (\omega_0/u_*\to 0)$$

(2) A general Formula of Transport Equation and its Application

Substituting eq. (50) into eq. (39) gives

$$\frac{\partial c}{\partial t}+U\frac{\partial c}{\partial x}=\beta_1-\beta_2 c \qquad \cdots\cdots(53)$$

in which β_1 and β_2 are described as follows:

$$\beta_1=\frac{1}{A}\frac{\rho_s}{\rho}p_{fs}q_s \qquad \cdots\cdots(54)$$

$$\beta_2=\frac{1}{A}\chi(\omega_0/u_*)(e_s q_s+2\lambda_s h V_{es}+\lambda_b B V_{eb}) \qquad \cdots\cdots(55A)$$

In case of $B\gg 2h$, β_2 reduces to

$$\beta_2=\frac{1}{A}\chi(\omega_0/u_*)(e_s q_s+\lambda_b B V_{eb}) \qquad \cdots\cdots(55B)$$

In case that U, β_1 and β_2 are without changes, eq. (53) can be solved, and then its solutions are

$$c(t,\ x)=c_0(t-x/U)e^{-\beta_2 x/U}+\beta_1/\beta_2\cdot(1-e^{-\beta_2 x/U}), \quad (\beta_2\neq 0) \qquad \cdots\cdots(56A)$$

and

$$c(t,\ x)=c_0(t-x/U)+\beta_1 x/U, \quad (\beta_2=0) \qquad \cdots\cdots(56B)$$

Flume experiments were carried out to test eqs. (53) and (56) within the artificial flume, which had erodible banks and beds composed of fine and coarse grains. Experimental methods and results have been published already (Ashida, Egashira

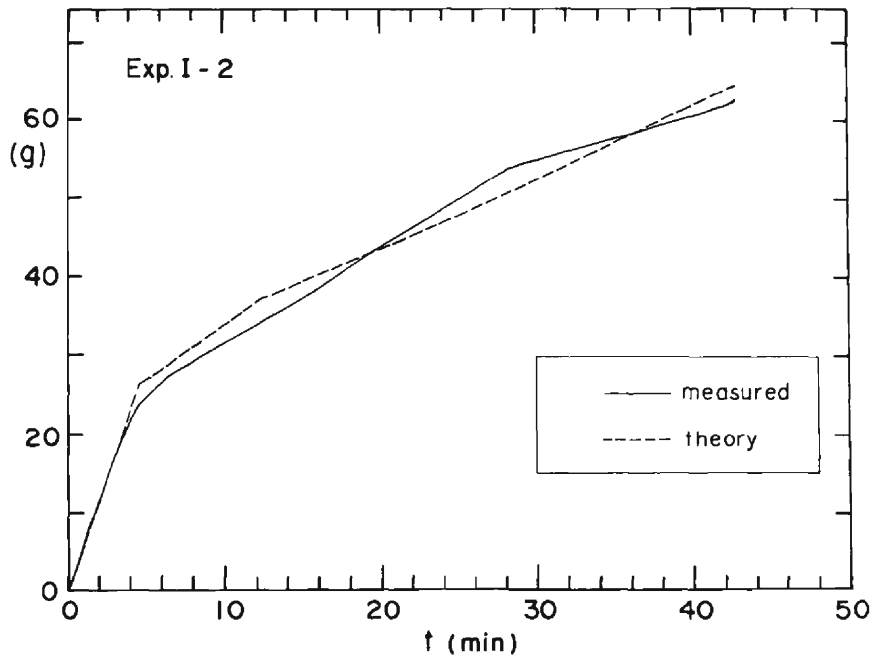

Fig. 17 The comparison between calculation and experiment with respect to the concentration of fine sediments due to bank erosion.

et al,[12] (1980). Therefore, we show a part of the results and compare it with the theory. In **Fig. 17**, experimental and theoretical curves associated with accumulated quantities of fine sediments washed out from the flume end are shown in gram units. Comparison between the two in the figure says that the theory presented here shows a good agreement with the experimental results.

5. A Model for Prediction of Fine Sediment Concentration

Problems concerning the producible regions of fine sediments, yield and transport mechanisms there and sediment concentration due to erosion and mixing action have been discussed hitherto. Therefore, if one makes a relevant model of the river basin and runoff model, a method to calculate the fine sediments concentration could be developed.

5.1 Modeling a Drainage Basin and Runoff Model

(1) Modeling a Drainage Basin

Criterions and methods for model-making should be chosen properly in accordance with the aim of study. The criterions of the present study should be taken as follows.

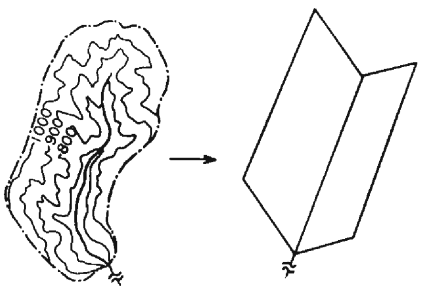

Fig. 18 A simulation of the unit basin.

(A) Any channel section in the drainage basin under consideration corresponds with that in the simulated basin one to one.

(B) Conditions of bare slopes formed in the actual basin can be evaluated directly in the simulated basin.

(C) Distribution of runoff discharge due to a rainfall can be calculated at any time and space in the simulated basin.

As a simulated basin satisfying the criterions mentioned above, the basin proposed by Sueishi[14] (1958) is considered sutable to the present study. Sueishi's model is as shown in **Fig. 18**. Using this model, a real basin is transformed into one stream channel and two parallelograms attached to both sides of it, which can be called "the unit simulated basin". Consequently, a whole river basin can be represented by series and parallel combinations of the unit simulated basin.

It is also an important problem how to determine the size of a real unit basin, because a free choice of the size brings some confusion.

The inclination angle of stream channel offers information to the determination of the size of a unit basin, because the phases of sediment yield is mainly subject to it in a crude sense. According to Takahashi's[15] (1980) theory, sediments which were deposited on the bed of slope angle grater than about fifteen degrees will be transported as a mud debris flow. Therefore, this critical angle θ_c gives a criterion to determine the size of a unit basin, because the phase of sediment yield due to mass movement should be excluded in the present study. The criterion is chosen consequently as follows:

(D) Streams which posess a slope greater than θ_c are excluded from the group classified as stream channel, while such streams are included as part of the parallelogram of the unit basin.

If one takes (D) into consideration in simulating the unit basin, the size of it could be determined. Then, the simulation of the drainage basin under consideration can be developed by combining the unit simulated basin.

(2) Runoff Model

(a) The Runoff Model at a Bare Slope

Yield and transport of fine sediments from a single gully have been discussed in Chap. 3. In order to calculate their yield from a bare slope, one need to know the number of gullies formed there, their length and flow discharge within the gullies. Then, the following suppositions are set forth here.

(A) A bare slope can be described by a rectangular form; its length and width are a_j and b_j respectively, and its inclination angle is θ_b.

(B) N_j gullies are formed in equal spacing on the bare slope, and their lengths are a_j.

Thereupon, the width of catchment area of a single gully could be written by

$$b_j' = b_j / N_j \qquad \cdots\cdots(57)$$

The lateral inflow rate q_g in unit time and length is described approximately by

$$q_g = b_j' \ (r - f_b') \cos\theta_b \qquad \cdots\cdots(58)$$

in which r is the intensity of a rain fall and f_b' infiltration capacity of the bare slope. Consequently, the discharge flowing down within the gully is expressed as

$$Q_g = Q_{g0} + \{b_j'(r - f_b') \cos\theta_b\} x_g \qquad \cdots\cdots(59)$$

in which Q_{g0} is the inflowing discharge from the upper end of the gully and x_g the distance along the gully. In eq. (59), it is a good approximation to suppose $Q_{g0}=0$.

As can be seen in the descriptions stated above, N_j which is the number of gullies formed on a bare slope is an important parameter to be determined by empirical method. Some discussions about it will be made in the next chapter.

(b) The Runoff Model to Predict the Discharge at Stream Channels

Various runoff models have been presented up to this time. However, they are not necessarily applied to the present study, because it is required to evaluate the flow discharge at any section of stream channel. Taking this stipulation into consideration, the kinematic wave runoff model for surface and subsurface flows proposed by Takasao[16] (1963) is thought to be pertinent here. This model is as follows. Formulas of surface runoff;

$$\frac{\partial h_1}{\partial t} + \frac{\partial q_1}{\partial x} = (r - f_1) \cos\theta_s \qquad \cdots\cdots(60)$$

$$h_1 = K_1 q_1^{\alpha_1} \qquad \cdots\cdots(61)$$

in which h_1 is the depth of surface runoff, q_1 the discharge of surface runoff, f_1 infiltration capacity of slope of unit model basin, θ_s inclination angle of the slope, $\alpha_1=0.6$, $K_1=n'^{0.6}\ (\sin\theta_s)^{-0.3}$ and n' equivalent roughness. Formulas of subsurface runoff;

$$\lambda_e \frac{\partial h_2}{\partial t} + \frac{\partial q_2}{\partial x} = (f_1 - f_2) \cos\theta_s \qquad \cdots\cdots(62)$$

$$h_2 = K_2 q_2 \qquad \cdots\cdots(63)$$

in which h_2 is the depth of subsurface runoff, λ_e the effective porosity, f_2 infiltration capacity between A-layer and the lower one, $K_2=1/k' \sin\theta_s$ and k' coefficient of permeability of A-layer. Formulas of flow discharge at channels;

$$\frac{\partial A}{\partial t} + \frac{\partial Q}{\partial x} = q_3 \sin\theta_3 \qquad \cdots\cdots(64)$$

$$A = K_3 Q^{\alpha_3} \qquad \cdots\cdots(65)$$

in which A is the cross sectional area of stream channel, Q flow discharge, θ_3 the angle of intersection of the stream cannel and the direction of lateral inflow, α_3 and K_3 coefficients associated with kinematics of stream flow and the shape of cross section, and $q_3 \sin\theta_3$ the lateral inflow rate in unit time and length. q_3 is described by

$$q_3 = q_1 + q_2 \qquad \cdots\cdots(66)$$

From these equations, which contain various parameters to be determined from field investigation, flow discharge along stream channels due to a rain fall can be calculated.

5.2 Yield and Transport Model of Fine Sediments in Mountainous Drainage Basins

(1) Modification of the Transport Formulas

(a) Modification of Eq. (25)

The yield and transport of fine sediments from a single gully was discussed already in the case that the flow discharge is unchanged along the flow direction. But as can be seen in eq. (59), the discharge due to rain fall changes both in time and space within a gully. This point should be taken into consideration, and moreover it should be specified which erosion process of the two prevails at the bare slopes.

In respect to the latter, it is supposed that an erosion process of weak soil layer is usually taking place during a rain, because the surface layer might be disturbed by the rain drops and the erodibility is kept high. Therefore, the yield of fine sediments from a single gully can be deduced in the same manner as discussed in Chap. 3. Using eqs. (16) and (26A) gives G_w.

$$G_w(t) = \rho_s(1-\lambda_1) p_{f1} \int_0^{a_j} E_{1*} u_* S_p dx_g \qquad \cdots\cdots(67)$$

in which G_w is the mass quantity produced from a single gully with a_j in length. For simplicity, S_p, which is the length of a wetted perimeter, is supposed to be

$$S_p \fallingdotseq B_g \qquad \cdots\cdots(68)$$

Shear velocity can be expressed as

$$u_* = (g \sin\theta_b / \varphi B_g) Q_g^{1/3} \qquad \cdots\cdots(69)$$

in which φ is the velocity factor defined by $\varphi = U/u_*$. Substituting eqs. (68) and (69) into eq. (67), and using eqs. (27) and (59) gives

$$G_w(t) = \frac{3}{5} \alpha'^{2/3} \rho_s (1-\lambda_1) p_{f1} E_{1*} \left(\frac{g \sin\theta_b}{\varphi} \right)^{1/3} \frac{\{a_j b_j'(r - f_b') \cos\theta_b\}^{2/3}}{b_j'(r - f_b') \cos\theta_b} \qquad \cdots\cdots(70)$$

Consequently, the yield of fine sediments with respect to one bare slope in which N_j gullies are formed is expressed as

$$G_{wt,j}(t)=N_jG_w(t)$$
$$=\frac{3}{5}a'^{2/3}\rho_s(1-\lambda_1)p_{f1}E_{1*}\left(\frac{g\sin\theta_b}{\varphi}\right)^{1/3}$$
$$\cdot\{(r-f_b')\cos\theta_b\}^{2/3}(a_jb_j)^{2/3}a_j(b_j/b_j')^{1/3} \quad \cdots\cdots(71)$$

in which suffix-j means the bare slope labeled "j".

(b) Modification of Parameters in Eq. (53)

In eq. (53), β_1 and β_2 describe the source and sink effects on the yield and transport of fine sediments, respectively. These formulas are rewritten below.

$$\beta_1=\frac{1}{A}\frac{\rho_s}{\rho}p_{fs}q_s \quad \cdots\cdots(54)$$

$$\beta_2=\frac{1}{A}\chi(\omega_0/u_*)(e_sq_s+\lambda_bBV_{eb}) \quad \cdots\cdots(55B)$$

On applying these formulas to practical probelms, it is important in particular how to evaluate the bank erosion and exchange velocity at stream channels. The former problem is discussed first and then the latter.

In most cases, the rate of bank erosion q_s is studied under the condition that left and right banks are formed by erodible materials. While in real streams, banks are not necessarily erodible everywhere, and base rocks or nonerodible areas are formed somewhere in stream channels. Therefore, the distribution density function is introduced in order to deal well with such a problem. The function is defined by

$$f_t(x)=(l_l+l_r)/\Delta x,\ (0\leqq f_t(x)\leqq 1) \quad \cdots\cdots(72)$$

in which l_l and l_r are the length of erodible left and right banks occupied along Δx.

Application of this function to q_s gives q_s' which is the rate of bank erosion at a real stream:

$$q_s'=f_t(x)q_s \quad \cdots\cdots(73)$$

A formula with respect to q_s has been presented by Muramoto, Tanaka and Fujita[17] (1972);

$$q_s=N_1(\tau_*'-\tau_{*c})u_*'d_m \quad \cdots\cdots(74)$$

in which u_*' is the shear velocity at the bank region, τ_*' nondimensional tractive stress defined by $\tau_*'=u_*'^2/(\rho_s/\rho-1)gd_m$, τ_{*c} the threshold of nondimensional tractive stress defined by Shields diagram, d_m mean diameter of bank materials and N_1 an empirical constant to be determined by experiments, and then u_*' is estimated by $u_*'=0.75\,u_*$ in which u_* is the shear velocity in cross-sectional mean.

It is well known that the formation and destruction of armour coats occur repeatedly in accordance with the rising and lowering stages of floods. It is likely that bank erosion cannot start untill the armour coat is destroyed. Therefore, this phenomenon should be taken into consideration with respect to eq. (74). In order to evaluate its effect on bank erosion, eq. (74) is reformed as follows.

$$q_s=\begin{cases}0 & (h\leqq h_c)\\ \dfrac{h-h_c}{h}N_1(\tau_*'-\tau_{*c})u_*'d_m, & (h>h_c)\end{cases} \qquad \cdots\cdots(75)$$

in which h is a flow depth and h_c the critical flow depth at which an armour coat is destroyed.

Secondly, brief discussions are taken in respect to eq. (55B). Mixing action between flowing water and pore water in the exchange layer of bed can occur only in movable beds. Therefore, we can evaluate the effect of exchange velocity, using the same distribution function as eq. (72):

$$f_b(x)=l_b/\Delta x,\ (0\leqq f_b(x)\leqq 1) \qquad \cdots\cdots(76)$$

in which l_b is the length of erodible bed existing in Δx. Therefore, using eq. (76) gives the modified exchange velocity:

$$V_{eb}'=f_b(x)V_{eb} \qquad \cdots\cdots(77)$$

From the above discussions the practical expressions of β_1 and β_2 are obtained. These are as follows.

$$\beta_1=\frac{1}{A}\frac{\rho_s}{\rho}p_{fs}f_t(x)q_s \qquad \cdots\cdots(78)$$

$$\beta_2=\frac{1}{A}\chi(\omega_0/u_*)\{e_sf_t(x)q_s+\lambda_bBf_b(x)V_{eb}\} \qquad \cdots\cdots(79A)$$

Substitution of eq. (41) into eq. (79A) reads

$$\beta_2=\frac{1}{A}\chi(\omega_0/u_*)\{e_sf_t(x)q_s+\lambda_bBf_b(x)V_{eb*}u_*\} \qquad \cdots\cdots(79B)$$

(2) Yield and Transport Model of Fine Sediments

Information necessary for making a hydraulic model for the prediction of wash load has been peresented by the above discussions.

Fig. 19 shows the bare slopes and small streams distributed over a unit drainage basin schematically. Small streams in the unit basin means "small" literally as discussed in 5.1, and they are not regarded as stream channel in the model. From the physical point of view, it is the fact that a stream channel flow is formed by the inflow from a smaller stream than itself. Therefore, the fine sediments produced at a bare slope inflow into a small stream first and then meet with the stream channel as shown in **Figs. 18** and **19**. Taking this matter into consideration, the following treatment might be possible. We turn our attention to the small stream meeting at x_i-point of stream

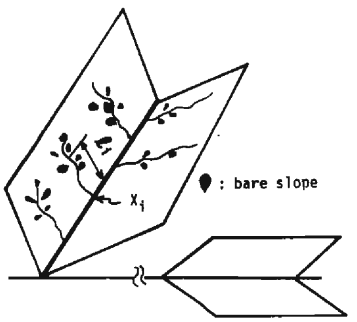

Fig. 19 A simulated unit basin and stream and bare slopes formed in the basin.

channel in **Fig. 19**, and suppose that n_i bare slopes exist in the small stream. Consequently, the total mass produced from all bare slopes in the small stream can be described by

$$\sum_{j=1}^{n_i} G_{wt,j}(t)$$

where $G_{wt,j}$ is defined by eq. (71). Besides, the propagation time of sediments from their production area to stream channel is supposed to be

$$t_d = l_i / u_s \qquad \cdots\cdots(80)$$

in which u_s is the velocity of lateral inflowing water of surface runoff and l_i is defined as

$$l_i = \sum_{j=1}^{n_i} a_j b_j l_j / \sum_{j=1}^{n_i} a_j b_j \qquad \cdots\cdots(81)$$

Consequently, the total mass produced from n_i bare slopes is written as

$$\sum_{j=1}^{n_i} G_{wt,j}(t-t_d)$$

Besides, using eq. (71) gives

$$\sum_{j=1}^{n_i} G_{wt,j}(t-t_d) = \sum_{j=1}^{n_i} \frac{3}{5} \alpha'^{2/3} \rho_s (1-\lambda_1) p_{f1} E_{1*} \left(\frac{g \sin\theta_b}{\varphi} \right)^{1/3}$$
$$\cdot [\{r(t-t_d) - f_b'\} \cos\theta_b]^{2/3} (a_j b_j)^{2/3} (b_j / b_j')^{1/3} a_j \qquad \cdots\cdots(82)$$

in which $r(t-t_d)$ is a rain fall intensity.

Combining eqs. (53), (64) and (82) and from discussions carried out hitherto, we obtain the formula with respect to the fine sediment concentration;

$$\frac{\partial c}{\partial t} + \frac{Q}{A} \frac{\partial c}{\partial x} = \beta_1 - \left(\beta_2 + \frac{1}{A} q_3 \sin\theta_3 \right) c$$
$$+ \delta(x - x_i) \frac{1}{A} \sum_{j=1}^{n_i} \frac{1}{\rho} G_{wt,j}(t-t_d)$$
$$(i = 1, 2, \ldots\ldots, N) \qquad \cdots\cdots(83)$$

in which $\delta(x-x_i)$ is the delta function defined by $\delta=1$ at $x=x_i$ and $\delta=0$ at $x \neq x_i$. Points in x-coordinate, where each small stream meets at the stream channel in the model unit basin, are as follows.

$$x_1, x_2, \ldots\ldots, x_i, \ldots\ldots, x_N$$

Moreover, the number of bare slopes in each small stream are described as

$$n_1, n_2, \ldots\ldots, n_i, \ldots\ldots, n_N$$

in which suffix-N means the number of small streams.

The following equations are applied to each term of eq. (83):

eqs. (60)~(66) with respect to Q and q_3;
eq. (78) with respect to β_1;
eq. (78A) or (79B) with respect to β_2;
eq. (82) with respect to $\sum_{j=1}^{n_t} G_{wt,j}(t-t_d)$.

The treatment concerning a unit drainage basin is as mentioned above. Regarding a whole drainage basin, the method applied to the unit basin is used either in parallel or series, or in both combinations (see **Fig. 21**).

6. Application of the Hydraulic Model to an Actual Basin

We will apply the model presented for the wash load to an actual problem and examine its utility. The Kawarabi river basin, the upstream region of Totsu river, is selected as the test basin.

For constructing the details of the model, some surveying and field experiments (see Chap. 3) were performed. The method and information are shown first, and then the discussions on the calculated results are presented.

6.1 Description of Kawarabi River Basin

(1) Division of the Basin

In the calculation, the basin is simulated with several unit basins such as described in **Fig. 19**. In order to simulate the Kawarabi basin, the slope angles and Horton-Strahler's stream orders of various stream branches were surveyed with 1/25000 maps according to the simulation method mentioned in 5.1. Then, the basin was finally divided into twelve unit basins as described in **Fig. 20** where Horton-Strahler's stream orders are shown schematically (see notation in the figure). Almost all slope angles of stream order 2 are evaluated to be larger than 15°. Consequently, referring to the criteria (D) in 5.1, the upstream end of river part of each unit basin is equivalent to the upstream end of a stream of order 3. The whole area of Kawarabi basin is simulated as shown in **Fig. 21**. The characteristic dimensions are summarized in **Table 3**, where A_d, L_s, θ_s and θ_3 indicate the area of slope region, the slope length measured perpendicularly to the stream channel, the slope angle of slope region and the angle of intersection of stream channel and the direction of lateral inflow, respectively. The upper and lower numerals in a frame correspond to the left and right banks, respectively.

(2) Investigation on the Production Areas of Fine Sediments

The sources of wash load are limited to bare slopes and erodible banks, as mentioned in Chap. 1. The basic data necessary for the calculation were obtained from utilizing maps, 1/10000 aerial photographs, field experiments and field surveys.

1509 bare slopes were found by inspecting maps and aerial photographs taken in 1976. The areas, the shapes, the number and the distribution of those bare slopes were evaluated by using aerial photographs, and their inclination angles

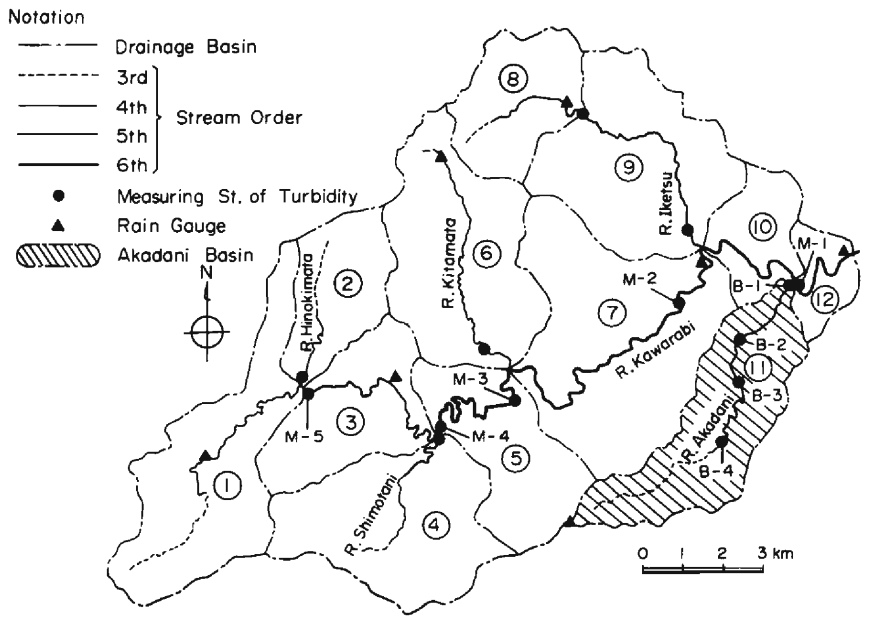

Fig. 20 A sketch of the Kawarabi river basin and measuring stations.

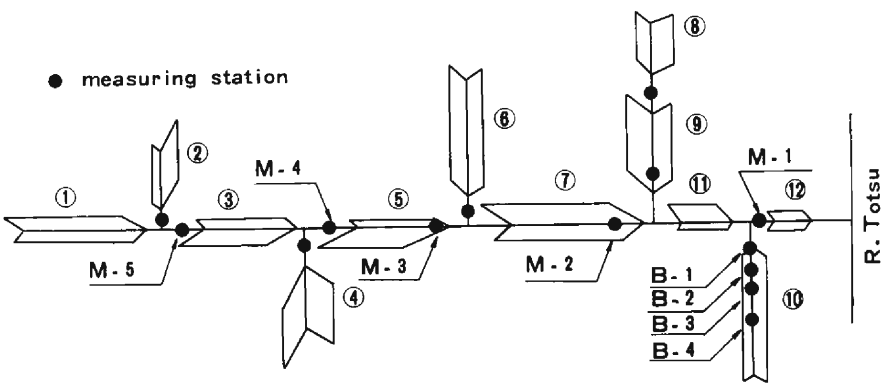

Fig. 21 The simulated Kawarabi river basin.

were determined with maps. Furthermore, field surveys on 73 typical bare slopes, corresponding to 5% of the total number, were performed with regard to the slope angles, the number of gullies, the cross-sectional profiles of gullies and particle size distributions of surface soil.

As discussed in Chap. 3, some field experiments were done to investigate the erodibility, flow resistance etc. on four typical bare slopes in the Akadani area. We obtained much precious field data which might be utilized in the consideration of the problems of other actual basins.

Parts of the results except those shown already in Chap. 3 are described below.

Table 3 Various factors of the Kawarabi river basin.

b. a. No.	A_d (km²)	L_s (km)	$\sin\theta_s$	$\sin\theta_3$	A_b (km_2)	A_b/A_d (%)	L_{ch} (km)	I	K_3	α_3	$\overline{f_t}$	d_{90} (cm)	h_c (cm)
1	10.114 8.512	2.14 1.35	0.375 0.391	0.500 0.699	0.0499	0.29	9.37	0.0192	1.177	0.627	0.48	10	27
2	6.164 2.536	2.75 0.70	0.391 0.423	0.485 0.788	0.0418	0.52	4.58	0.0434	0.781	0.639	0.19	15	17
3	4.204 7.841	1.14 2.46	0.485 0.407	0.545 0.469	0.0711	0.66	6.74	0.0127	1.429	0.621	0.24	9	34
4	8.179 10.182	3.64 2.44	0.485 0.423	0.454 0.857	0.0710	0.43	4.87	0.0587	0.767	0.631	0.09	25	21
5	3.045 10.379	1.12 4.07	0.500 0.485	0.497 0.391	0.0327	0.28	6.68	0.0112	1.572	0.615	0.14	10	46
6	9.678 10.322	1.45 1.66	0.423 0.454	0.777 0.719	0.0605	0.34	8.65	0.0333	0.922	0.628	0.16	18	27
7	14.669 13.245	3.07 2.03	0.515 0.485	0.485 0.656	0.2605	1.08	9.85	0.0151	1.615	0.609	0.23	15	49
8	6.561 3.657	1.91 1.54	0.391 0.342	0.914 0.629	0.0500	0.54	3.78	0.0312	1.156	0.616	0.24	22	29
9	8.585 10.903	1.69 2.52	0.454 0.469	0.866 0.743	0.0713	0.41	5.86	0.0400	0.922	0.622	0.12	22	29
10	7.153 9.905	0.95 1.21	0.545 0.485	0.755 0.819	0.1045	0.71	10.00	0.0624	0.887	0.621	0.43	20	16
11	4.982 1.696	1.85 0.83	0.496 0.574	0.719 0.559	0.0357	0.62	3.72	0.0108	2.067	0.615	0.48	11	49
12	1.641 2.384	1.02 1.13	0.574 0.530	0.574 0.743	0.0611	1.81	2.83	0.0106	1.993	0.612	0.44	12	57

Table 4 Geometric shape factors of bare slopes.

$A_{b,j}=a_jb_j$ \ a_j/b_j	0.38～1	1～5	5～10	10～85
100～ 500 m²	4(0)	516(24)	486(46)	59(13)
500～ 1000	4(1)	94(5)	136(7)	60(19)
1000～ 1500	3(0)	31(3)	21(3)	15(3)
1500～ 2000	1(0)	9(0)	8(1)	12(2)
2000～38800	6(2)	25(2)	18(5)	1(0)

The area of bare slope A_b and bare slope ratio A_b/A_d in each unit basin are tabulated in the sixth and seventh columns of **Table 3**. In **Table 4**, the distribution of the number of bare slopes is shown with respect to the shapes and areas, where the numbers in the brakets belong to the Akadani basin (see **Fig. 20**). **Fig. 22**

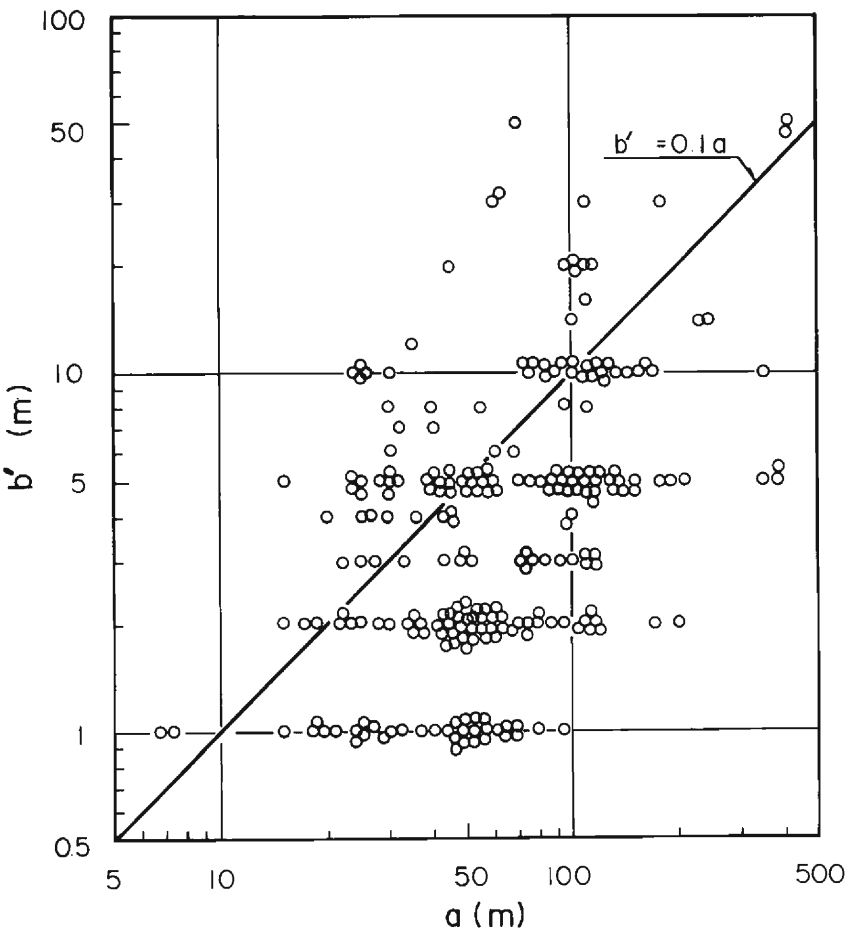

Fig. 22 The relation between the width of catchment area of a single gully and the length of a bare slope.

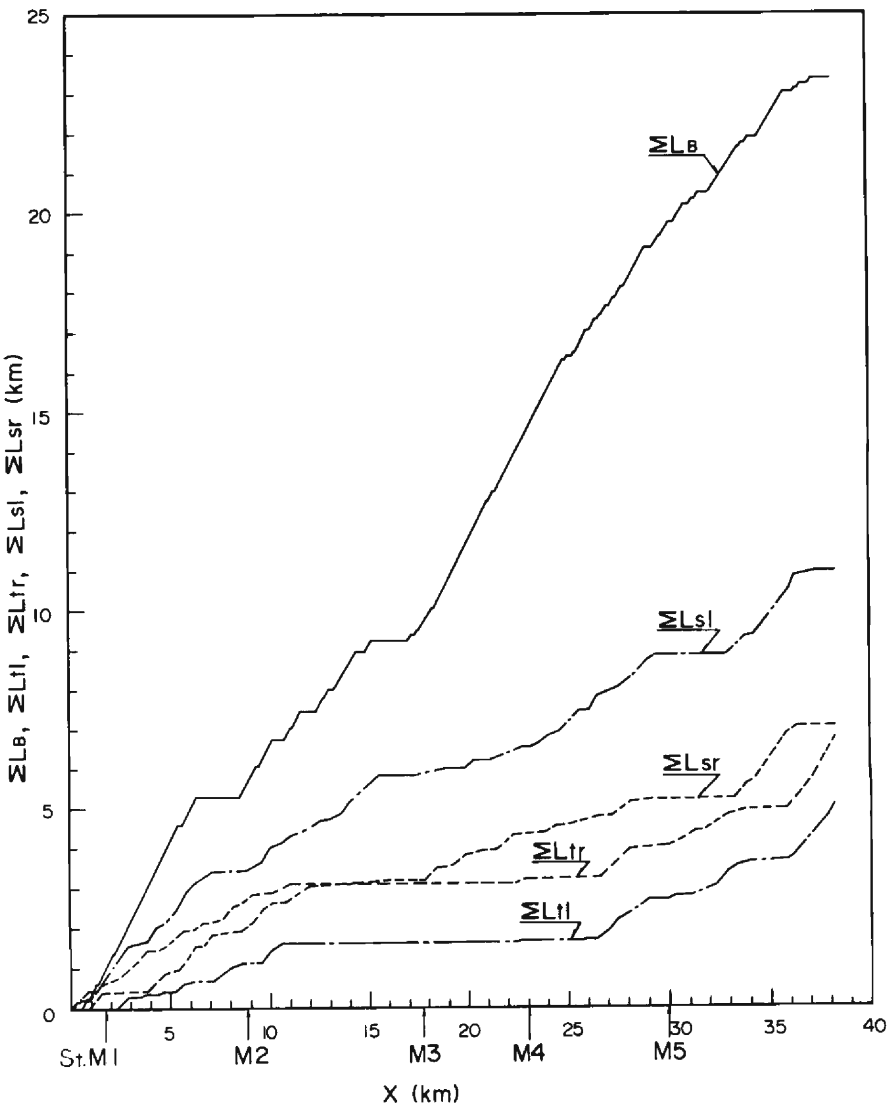

Fig. 23 The accumulated lengths of erodible banks and beds in stream channels vs. those of stream channels in the Kawarabi river basin.

shows the relation between the length a_j of bare slope and the width b_j' of the catchment area of a single gully. From a practical view point, the relation may be expressed by

$$b_j' = 0.1\, a_j \qquad \cdots\cdots(84)$$

While, various investigations associated with the stream channels and channel deposits were carried out. Longitudinal and transverse cross sections, distributions of erodible banks and beds, and grain size distribution were surveyed and investi-

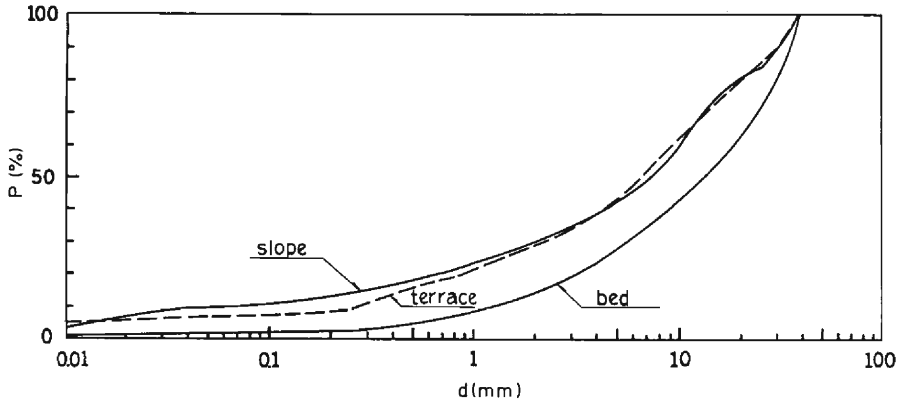

Fig. 24 The grain size accumulation curves at production regions of fine sediments in the Akadani river basin.

gated along the Akadani river. Data concerning L_{ch} (length of stream channel of unit basin), I (slope of stream channel), K_3, α_3, $f_t(x)$, $f_b(x)$, p_{fs}, d_{90} (90% diameter in grain size distribution curves) and so on were obtained from these investigations.

For example, the results with respect to $f_t(x)$ and $f_b(x)$ along the main of Kawarabi river are presented in **Fig. 23**. In the figure, $\sum L_{sl}$ and $\sum L_{sr}$ indicate the accumulated length of land slide regions along the left and right river banks, $\sum L_{tl}$ and $\sum L_{tr}$ those of the terraced and man-made sediments along the both sides of river channel, and $\sum L_b$ those of the bed sediments. According to eqs. (72) and (76), $f_t(x)$ and $f_b(x)$ are determined as follows.

$$f_t(x)=\frac{1}{2\Delta x}\sum_{x}^{x+\Delta x}(L_{sl}+L_{sr}+L_{tl}+L_{tr}) \qquad \cdots\cdots(85)$$

$$f_b(x)=\frac{1}{\Delta x}\sum_{x}^{x+\Delta x}L_B \qquad \cdots\cdots(86)$$

In **Fig. 24**, particle size distribution curves investigated in the Akadani basin are shown, where "slope" means the datum of bare slopes, "terrace" that of erodible banks and "bed" that of bed materials, and each datum is the arithmetic mean of several tens of data. According to the results shown in the figure, p_{fl}, p_{fs} and p_{fb}, which are the composition rates of fine sediments at bare slopes, erodible banks and bed, respectively, are estimated as follows.

$$p_{fl}=0.1,\ p_{fs}=0.6 \text{ and } p_{fb}=0.2$$

At the remaining unit basins, data required for the calculation of wash load were inferred from an extrapolation method and inspection of aerial photographs.

Some parts of the data obtained are tabulated in the columns from the eighth to thirteenth of **Table 3**, where $\bar{f}_t$ is the mean of $f_t(x)$ in the stream reach and h_c

is the water depth, at which the armour coat starts to be destroyed, calculated from the formula presented by Ashida and Michiue[18] (1972).

(3) Observation of Sediment Concentrations during a Runoff

Various observations during a flood occurring on June 26th~30th, 1979 were carried out at the measuring stations shown in **Fig. 20.**

Data concerning sediment concentrations and the particle sizes were obtained at stations (M–5, M–4, M–3, M–2, M–1 and B–1) through both the rising and falling stages of flood. From these data, it was found out that most particles suspended in flowing water were composed of finer grains than the maximum limit of fine sediments defined by the discussions in Chap. 1. Therefore, the measured sediment concentrations can be regarded as those of fine sediments. These data are compared later to the concentrations predicted by the model.

6.2 Application

Concentrations of fine sediments, in other words, sediment rating curves, can be predicted by eq. (83) and its supplementary equations with a digital computer if the distribution of rainfall intensities in time and space and some other factors associated with the bare slopes and drainage basin are known. The numerical methods used here are as follows; specific curve method as to flow discharge and a finite difference method in common use with respect to the concentration of fine sediments.

First, the comparisons between the prediction and observation are made with respect to the time changes of the concentration at each measuring station. **Figs. 25(a)~(e)** show the comparisons between the two at M–5, M–4, M–3, M–2

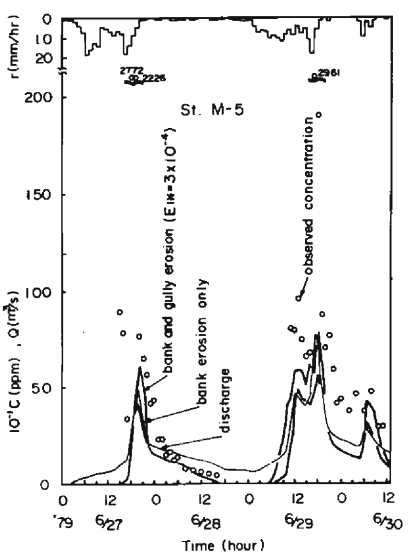

(a)

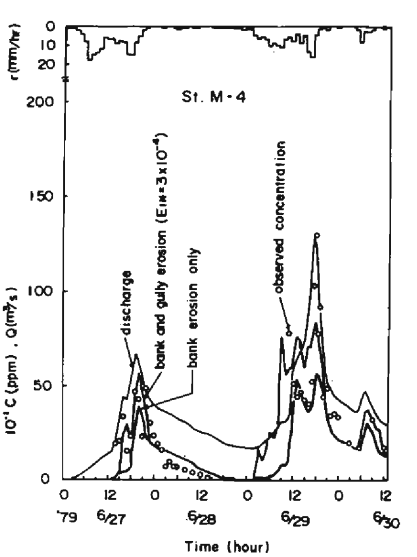

(b)

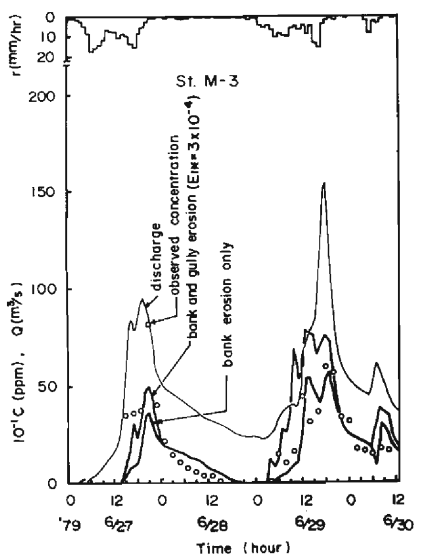

(c)

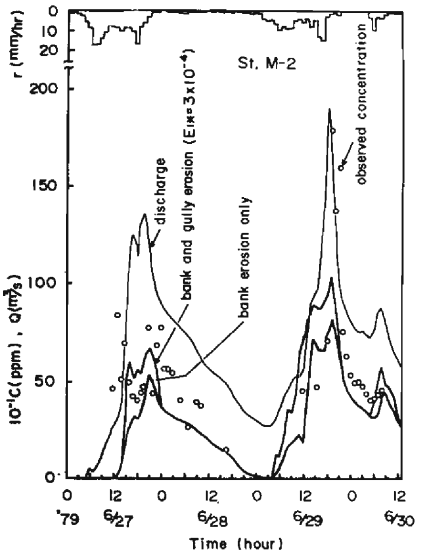

(d)

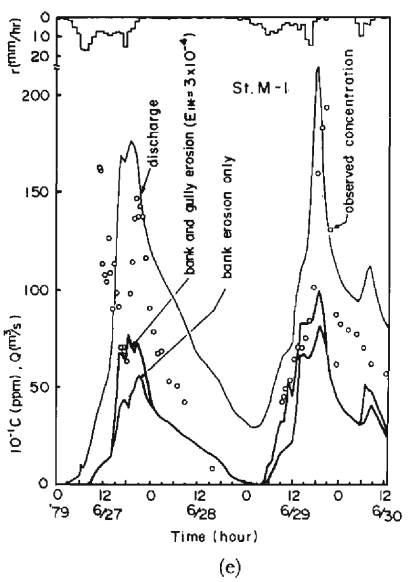

(e)

Fig. 25 The comparisons between predicted curves and observed data with respect to the concentrations of fine sediments vs. flow discharge

and M-1 along the main stream of Kawarabi river. In the figures the following are also shown; the distribution of rainfall intensity evaluated by Thiessen's method, curves of the calculated discharge, and curves of sediment concentration predicted under the assumption of $E_{1*}=0$ which means zero-production from bare slopes. Consequently, the curves with $E_{1*}=3\times10^{-4}$ minus those with $E_{1*}=0$ mean the yields from bare slopes only. "Predicted curve" is regarded as the one with $E_{1*}=3\times10^{-4}$.

Then, concentrating our eyes on the results of these figures, it is found that both the predicted curves and observed data change in accordance with hydrographs and in addition the latter are well predicted by the model, except for some data in **Fig. 25(e)**.

In this model, the beginning of the increase in sediment concentration is expressed in terms of the destruction of armour coat (see eq. 75) or the start of gully

erosion due to the formation of surface runoff. Inspecting the discharges with respect to the beginning of transport of fine sediments, we get the following: At M–5, M–4, M–3, M–2 and M–1,

10, 20, 20~30, 20~50 and 30~60 m^3/sec in the observation versus

10, 20, 20~30, 20~30 and 25~30 m^3/sec in the prediction, respectively.

On the other hand, the discharges at which armour coats start to be destroyed are as follows.

12.5, 22.3, 22.3, 37.0 and 54.5 m^3/sec

at each measuring station. These results show that the rising stage of sediment concentration can be predicted well by the model and moreover it is caused by the destruction of armour coat.

Secondly, investigation with respect to the relation of sediment concentration with flow discharge (C vs. Q-curve) is taken up. It has been understood that sediment concentrations do not correspond with flow discharges uniquely even in a flood, and C vs. Q-curves in rising and falling stages are different from each other. Such a phenomenon, which is a kind of hysteresis, might be caused by the following;

(a) change of rainfall intensity in time and space.
(b) change of runoff characteristic in time.
(c) change of erodibility of production areas in time.
(d) lag between the velocity of flowing water and celerity of flood wave.

In the present model, (c) of the four has not been taken into consideration. **Figs. 26(a)** and **(b)** show the results with respect to C vs. Q-relations at M–4 and M–2, respectively, where the arrows mean the time course. As can be seen in these figures, it is found that the observed data are predicted well by the present model as a whole.

Now we pay our attention to the effect of (b) mentioned above on C vs. Q-relations. As can be seen in the results of **Figs. 25(a)–(e)**, the flood referred to here has two peaks in flow discharge. Therefore, the runoff characteristics are different from each other in the first half and the latter half of the two runoffs, because the surface runoff is scarcely formed at the early stage of rainfall in the former, while surface runoff is formed in the later runoff as soon as it begins to rain again. Taking these descriptions into consideration and inspecting the C vs. Q-relations shown on the left and right of **Figs. 26(a)** and **(b)**, one can appreciate an impressive difference of C vs. Q-relations between the first half and the latter half of the runoff, especially in the rising stage of discharge. In C vs. Q-relation of the latter, sediment concentrations increase rapidly as soon as it begins to rain because the fine sediments due to gully erosions are added to the stream channel early in the rising stage.

7. Conclusion

Various problems concerning wash load during a runoff have been discussed, and a hydraulic model to calculate the concentration of wash load has been present-

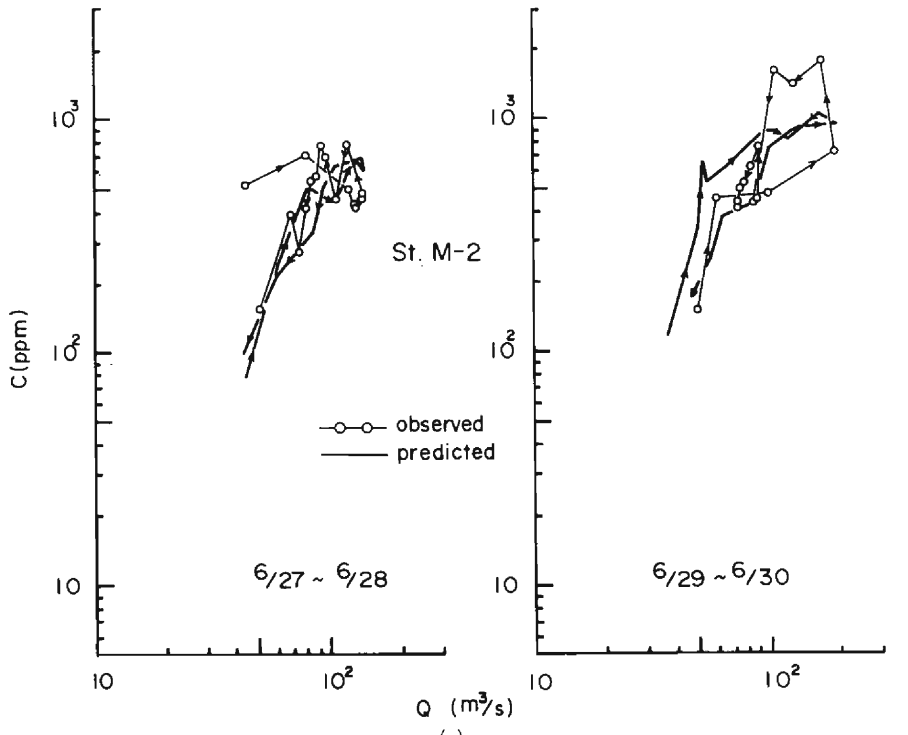

(a)

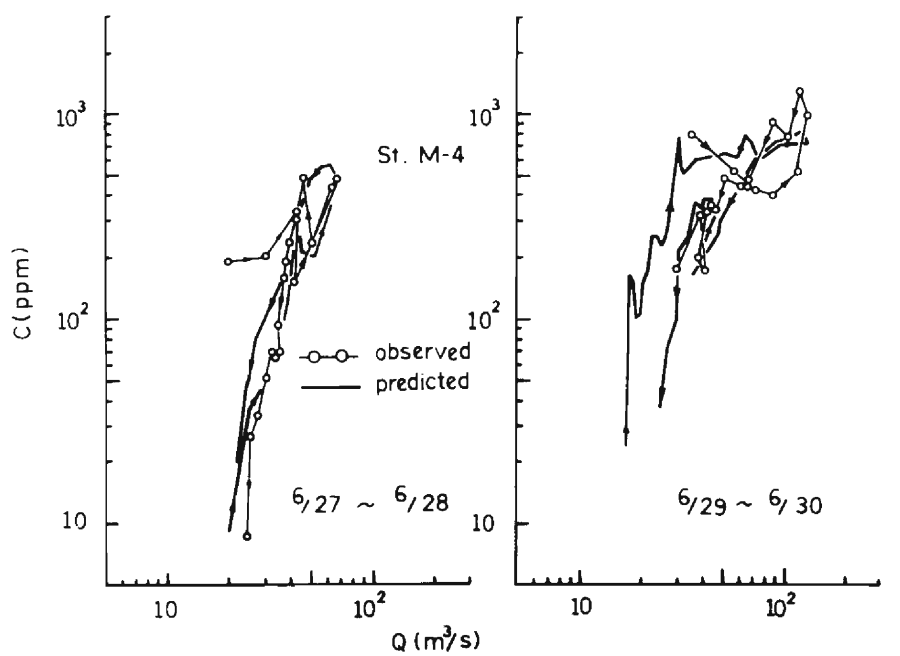

(b)

Fig. 26 The concentrations of fine sediments vs. flow discharge during the flood (C vs. Q-relation).

ed. The results obtained from the present study are as follows.

(1) The particle sizes with respect to wash load were discussed from sediment hydraulic points of view and field data, and then it is proposed that dealing with those finer than 100 μm in diameter is adequate for the purpose of the present study. Their production regions are specified as bare slopes and erodible banks.

(2) The erosion process is classified into the process of weak soil layer and that of strong soil layer, and in the former process erosion velocity is constant without armouring process. While in the latter, erosion ceases due to the formation of an armour coat. Yield and transport of fine sediments at bare slopes are formulated, supposing that the gully erosion is predominant at bare slopes.

(3) Yield and transport within stream channels were formulated, supposing that bank erosion and mixing action between flowing water near the bed and pore water in exchange layer are predominant. In the formula, the bank erosion is the sediment source, while mixing action acts as its sink generally.

(4) The simulation technique and its criteria of drainage basins were discussed and specified. Then the calculation method of flow discharge in stream channel was considered in the simulated basin and the method to predict flow discharge within a gully during a rainfall is proposed.

(5) A method of predicting the concentration of wash load or "fine sediments" was presented by combining the results from (1) to (4). We call the model "hydraulic model of wash load". According to the model, concentration of wash load can be predicted in any time and place of a drainage basin if distribution of rainfall intensity, distribution of the number and shapes of bare slopes, erodibility of bare slopes, kinematic and geometric factors of stream channels, and grain size distributions in bare slopes and stream channels are given.

(6) The model was applied to the Kawarabi river basin. It was found that the concentrations of wash load were calculated well at any cross section in the basin.

Acknowledgment

This study has been part of a research entitled "Yield and Transport of fine sediments in mountainous drainage basins" supported by the Science Research under the Ministry of Education. This support is gratefully acknowledged. We are also grateful to Mr. S. Furukawa for his help in calculation, and also grateful to staff of Ministry of Construction for their help in field investigation and observation.

References

1) Rendon-Herrero, O.: Estimation of wash load produced on certain small watersheds, Jour. Hydraulic Div., Proc. ASCE, Vol. 100. Hy7, 1974, pp. 835–848.
2) Muramoto Y., M. Michiue and E. Shimojima: On the transport processes of wash load in Daido River, Disast. Prev. Res. Inst. of Kyoto Univ. Annuals, No. 16B, 1973, pp. 433–447. (in Japanese)
3) Williams, J. R.: A sediment graph model based on an instantaneous unit sediment graph, Water Resources Research, Vol. 14, 1978, pp. 659–664.

4) Einstein, H. A., A. G. Anderson and J. W. Johnson: A distinction between bed-load and suspended load in natural streams, Trans. AGU, 1940, pp. 628–633.
5) Einstein, H. A. and Ning-Chien: Can the rate of wash load be predicted from the bed load function?, Trans. AGU, Vol. 36, 1953, pp. 876–882.
6) Kanayashiki, T., K. Ashida and S. Egashira: A hydraulic model of the yield of wash load in mountainous areas; Proc. 24th Jap. Con. on Hydraulics, 1980, pp. 143–151. (in Japanese)
7) Heidel, S. G.: The progressive lag of sediment concentration with flood waves, Trans. AGU, Vol. 37, 1956, pp. 56–66.
8) Egashira, S. and K. Ashida: Production region and yield process of fine sediments in mountainous drainage basins, Disast. Prev. Res. Inst., Kyoto Univ. Annu als, No. 24B–2, 1981, pp. 241–252. (in Japanese)
9) Ashida, K. and K. Sawai: Erosion and cross section on the cohesive stream bed, Bull. Disast. Prev. Res. Inst., Kyoto Univ., Vol. 26, Part 3, 1976, pp. 145–161.
10) Ashida, K., S. Egashira and T. Kanayashiki; On the yield of wash load by slope erosion, Proc. 24th Jap. Con. on Hydraulics, 1980, pp. 135–141. (in Japanese)
11) Ashida, K., A. Daido, T. Takahashi and T. Mizuyama: Study on the Resistance law and initiation of motion of bed particles in a steep slope channel, Disast. Prev. Res. Inst., Kyoto Univ. Annuals, No. 16B., pp. 481–494. (in Japanese)
12) Ashida, K., S. Egashira, T. Tadayoshi and Y. Ogawa: Yield processes of wash load in stream channels, Disast. Prev. Res. Inst., Kyoto Univ. Annuals, No. 23B-2, 1980, pp. 413–431. (in Japanese)
13) Zagni, A. F. E. and K. V. H. Smith: Channel flow over permeable beds of graded spheres, Jour. Hydraulic Div., Proc. ASCE, Vol. 102, No. Hy2, 1976, pp. 207–222.
14) Sueishi, T.: On the runoff analysis by specific curve method, Proc. JSCE, No. 29, 1955, pp. 77–87. (in Japanese)
15) Takahashi, T.: Mechanical characteristics of debris flow, Jour. Hydraulic Div., Proc. ASCE, Vol. 104. No Hy8, 1978, pp. 1153–1169.
16) Takasao, T.: Occurence area of direct runoff and its variation process, Disas. Prev. Res. Inst., Kyoto Univ. Annuals, No. 6, 1963, pp. 166–180. (in Japanese)
17) Muramoto, Y., S. Tanaka and Y. Fujita: Studies on fluvial process of stream channels (3), Disast. Prev. Res. Inst., Kyoto Univ. Annuals, No. 15B, 1972, pp. 385–404. (in Japanese)
18) Ashida, K., and M. Mchiue: Study on hydraulic resistance and bed-load transport rate in alluvial streams, Proc. JSCE, No. 206, 1972, pp. 59–69. (in Japanese)